Simulation of initial uncertainties using singular vectors (SVs) and an ensemble of analyses (EDA)

(EC/TC/PR/RB-L3)

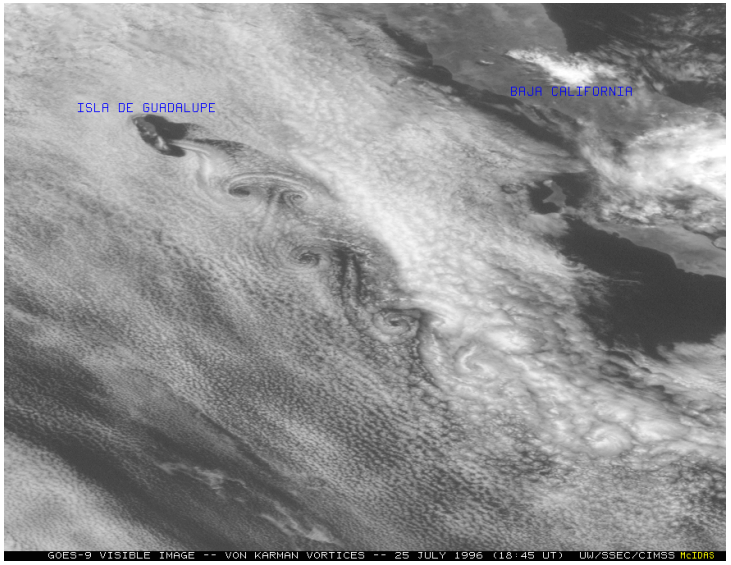

Roberto Buizza

European Centre for Medium-Range Weather Forecasts

(http://www.ecmwf.int/staff/roberto_buizza/)

Abstract and key learning points

The aim of this session is to introduce the ECMWF ensemble of data assimilation (EDA). The rationale and methodology of the EDA will be illustrated, and its use in to simulate initial uncertainties in the ECMWF ensemble prediction system (ENS) will be presented.

By the end of the session you should be able to:

- know what is the ECMWF EDA
- illustrate how the EDA is used to simulate initial uncertainty in ensemble prediction
- understand the main differences between singular vectors and EDA-based perturbations

Outline

1. The original SV-based ECMWF ensemble
2. Ensemble Data Assimilation characteristics
3. The EDA-SVINI ensemble

1. The operational ensemble in 2015

ENS includes 51 forecasts with resolution:

- T_L639L91 (~32km, 91 levels) from day 0 to 10
- T_L319L91 (~64km, 91 levels) from day 10 to 15 (32 at 00UTC on Mon and Thu).

Initial uncertainties are simulated by adding to the unperturbed analyses a combination of T42L91 singular vectors, computed to optimize total energy growth over a 48h time interval (OTI), and perturbations generated by the ECMWF Ensembles of Data Assimilation (EDA) system.

Model uncertainties are simulated by adding stochastic perturbations to the tendencies due to parameterized physical processes (SPPT and SKEB schemes).

The unperturbed analysis is given by the T_L1279L137 4DVAR.

ENS runs daily at 00 and 12 UTC, with a TOA at 0.01 hPa.

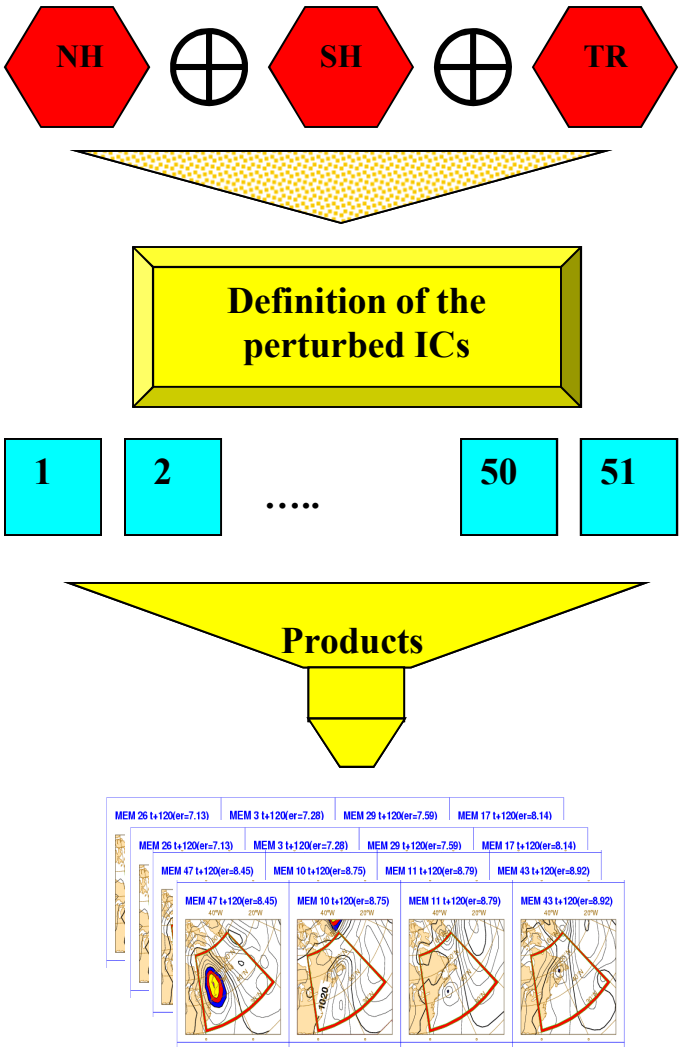

1. The original ENS (before 2010)

Each ensemble member evolution is given by the time integration

$$e_j(d,T) = e_j(d,0) + \int_0^T [A(e_j,t) + P(e_j,t) + \delta P_j(e_j,t)]dt$$

of perturbed model equations starting from perturbed initial conditions

$$e_j(d,0) = e_0(d,0) + de_j(d,0)$$

$$de_j(d,0) = \sum_{area} \sum_{k=1}^{N_{SV}} [\alpha_{j,k} \cdot SV_k(d,0) + \beta_{j,k} \cdot SV_k(d-2,+2d)]$$

The model tendency perturbation is defined at each grid point by

$$\delta P_j(e_j,t;\lambda,\phi,p) = r_j(t;\lambda,\phi) P_j(t;\lambda,\phi,p)$$

where $r_j(t;\Phi,\lambda)$ is a random number.

1. The original ENS (before 2010)

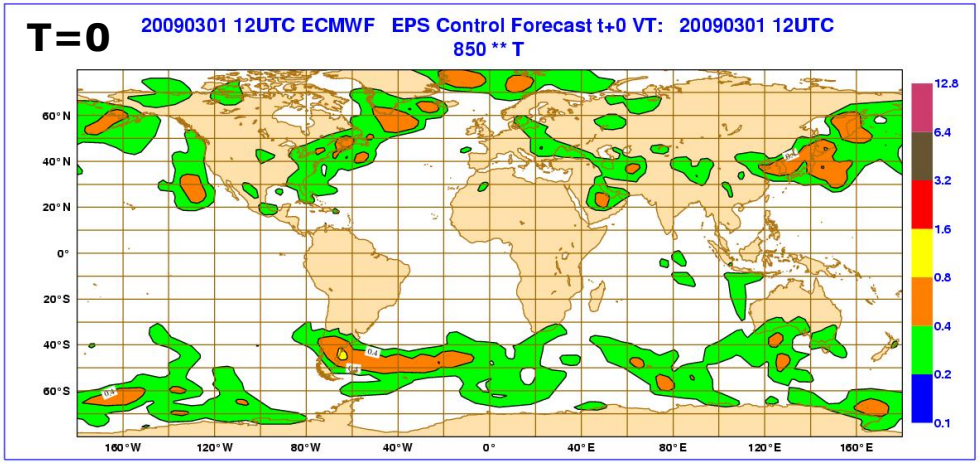

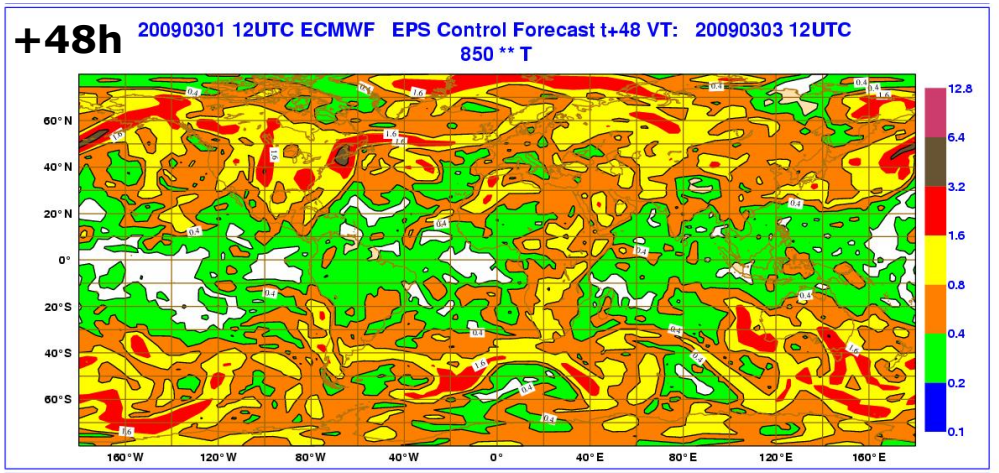

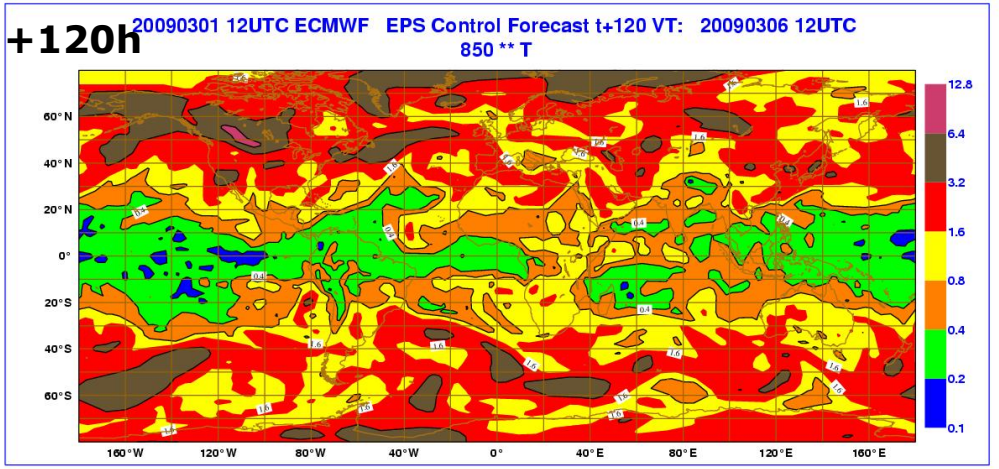

The initial perturbations do not sample the tropics in an appropriate way. The system is not 'reliable' (spread under estimation).

1. std/EM of ECMWF 399v255 and 639v319 ENS

NH: apart for the first 2 days the spread-skill relationship is very good, with the 639v319 version (implemented in Jan 2010) showing a better match.

Tropics: both systems are under-dispersive for the whole forecast range.

Is this a symptom of a weakness of the initial perturbation strategy?

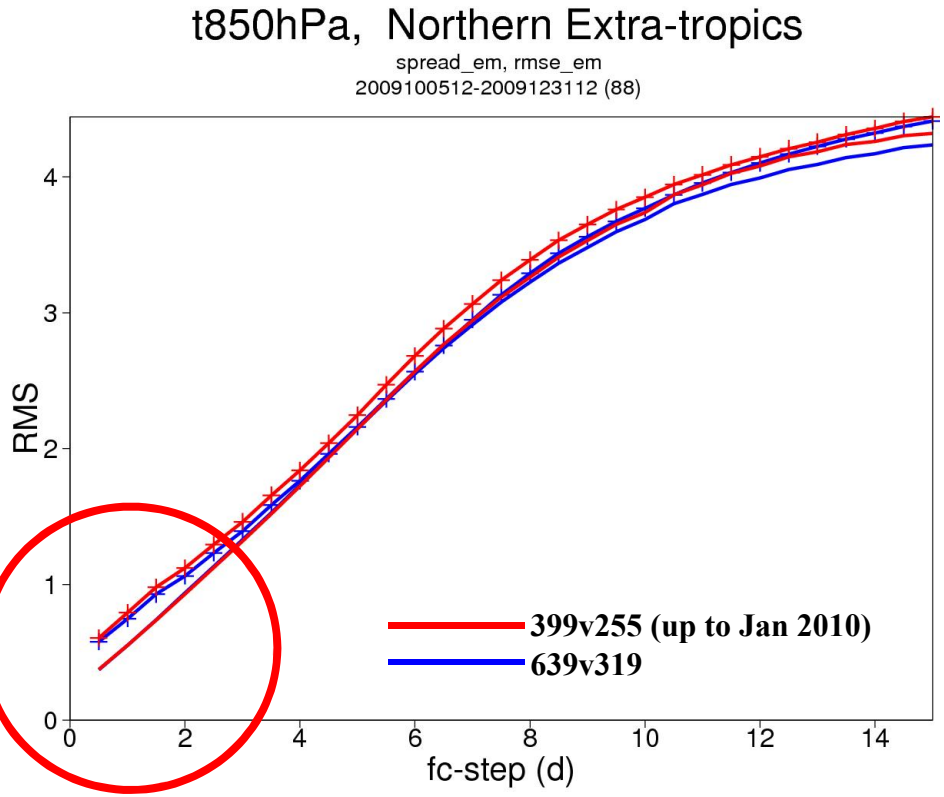

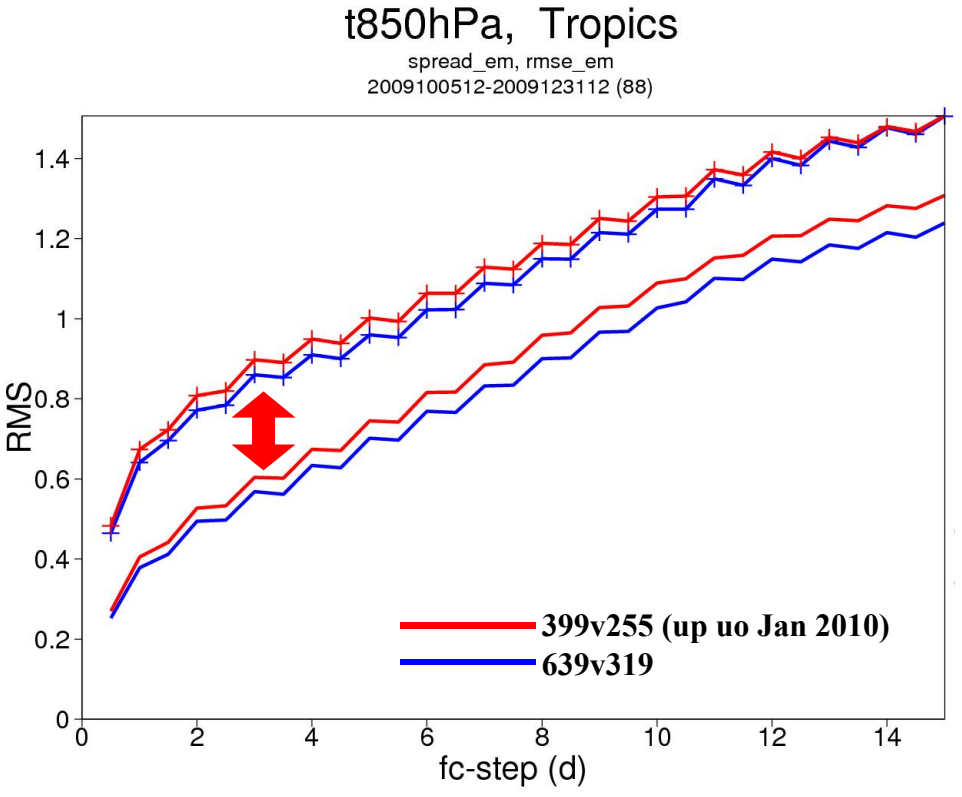

1. The TIGGE ensembles (updated Nov 2014)

The 9 TIGGE operational, medium-range, global ensembles use different methodologies to simulate initial-time and model uncertainties. Every day, the 7 ensembles that are still operational, put 436 forecasts into the TIGGE archive. These forecasts have horizontal resolution ranging from about 210 km to about 32 km, and forecast length between 10 and 16 days. They all simulate initial/observation and model uncertainties in different ways.

Centre	Initial unc. method (area)	Model unc.	Truncation (degrees, km)	# Vert Lev (TOA, hPa)	Fcst length (d)	# pert mem	#runs per day (UTC)	# mem per day	In TIGGE since
BMRC (AU)	SV(NH,SH)	NO	TL119 (1.5°; 210km)	19 (10.0)	10	32	2 (00/12)	66	Sep-07/Jul-10
CMA (CHI)	BV(globe)	NO	T213 (0.56°; 70km)	31 (10.0)	10	14	2 (00/12)	30	May-07
CPTEC (BR)	EOF(40S:30N)	NO	T126 (0.94°, 120km)	28 (0.1)	15	14	2 (00/12)	30	Feb-08
ECMWF (EU)	SV(NH, SH, TC) + EDA(globe)	YES	TL639 (0.28°; 32km) TL319 (0.56°; 65km)	91 (0.1)	0-10 15/32	50	2 (00/12)	102	Oct-06
JMA (JAP)	SV(NH, TR, SH)	YES	TL479 (0.38°; 50km)	60 (0.1)	11	25	2 (00/12)	52	Aug-11
KMA(KOR)	ETKF(globe)	YES	N320 (0.35°; 40km)	70 (0.1)	10	23	4 (00/06/12/18)	96	Dec-07
MSC (CAN)	EnKF(globe)	YES	600x300 (0.6°, 75km)	40 (2.0)	16/32	20	2 (00/12)	42	Oct-07
NCEP (USA)	ETR(globe)	YES	T254 (0.70°; 90km) T190 (0.95°; 120km)	28 (2.7)	0-8 8-16	20	4 (00/06/ 12/18)	84	Mar-07
UKMO (UK)	ETKF(globe)	YES	N216 (0.45°; 60km)	70 (0.1)	15	23	2 (00/12)	48	Oct-06/Jul-14

Outline

1. The original SV-based ECMWF ensemble
2. Ensemble Data Assimilation characteristics
3. The EDA-SVINI ensemble

2. The ECMWF 4D-Var data-assimilation system

The ECMWF 4-dimensional data-assimilation system determines a correction to the background initial condition (blue line) that would lead to a forecast trajectory (red line) that passes closer to the observations (red circles).

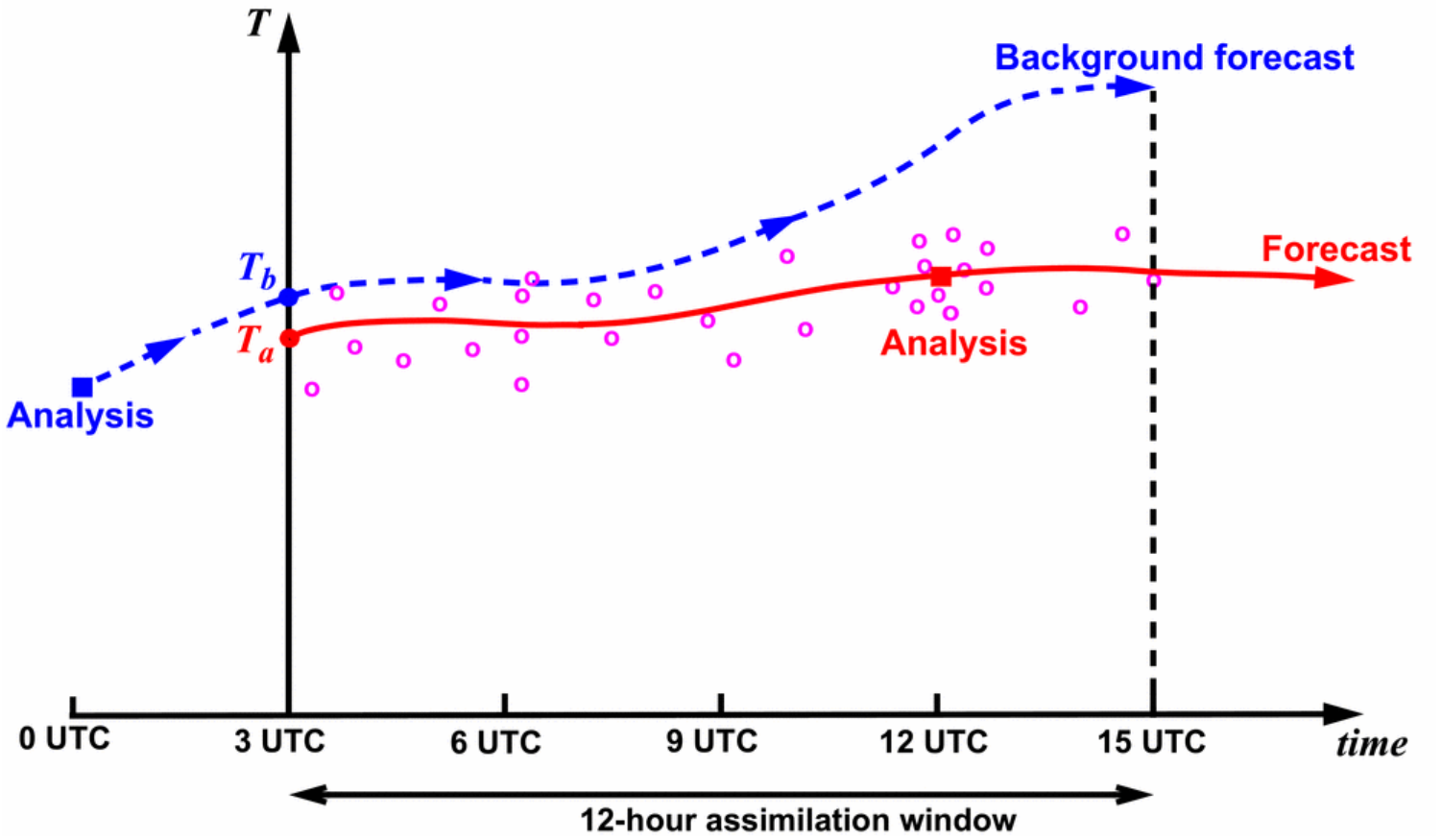

2. The ECMWF EDA

Each observation has an error (instrument, representativeness) and model error should be taken into account. A way to simulate both these effects is to run an ensemble of assimilations.

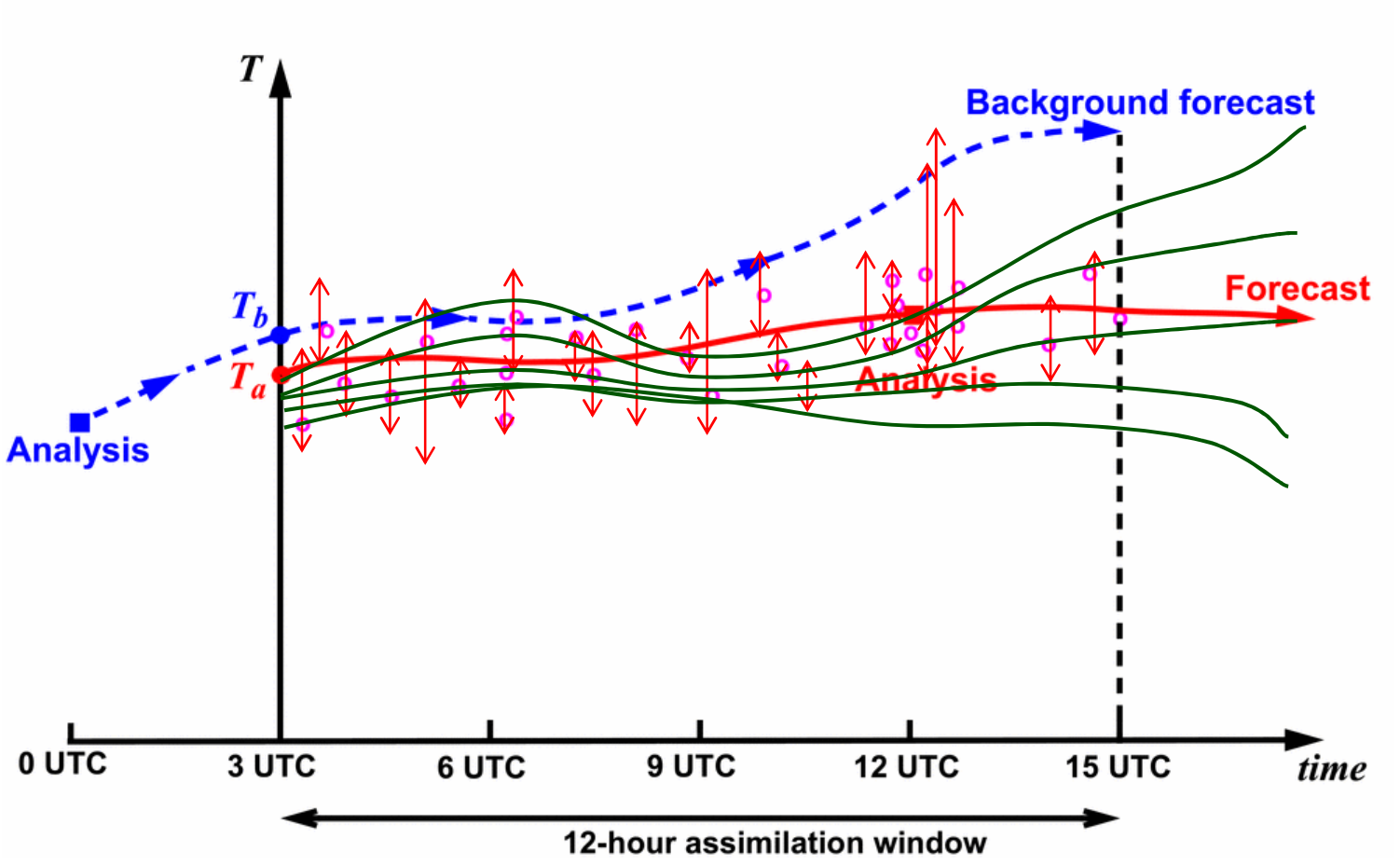

2. Ensemble Data Assimilation and Prediction

- The EDA analyses are generated by randomly perturbing the observations and the SST; the observations are assumed unbiased, with obs-error std defined by a normal distribution
- Model error is simulated using stochastic schemes
- Differences between pairs of analyses (and forecast) fields have the statistical characteristics of analysis (and forecast) error.
- The EDA analyses can be used to specify flow-dependent background error statistics

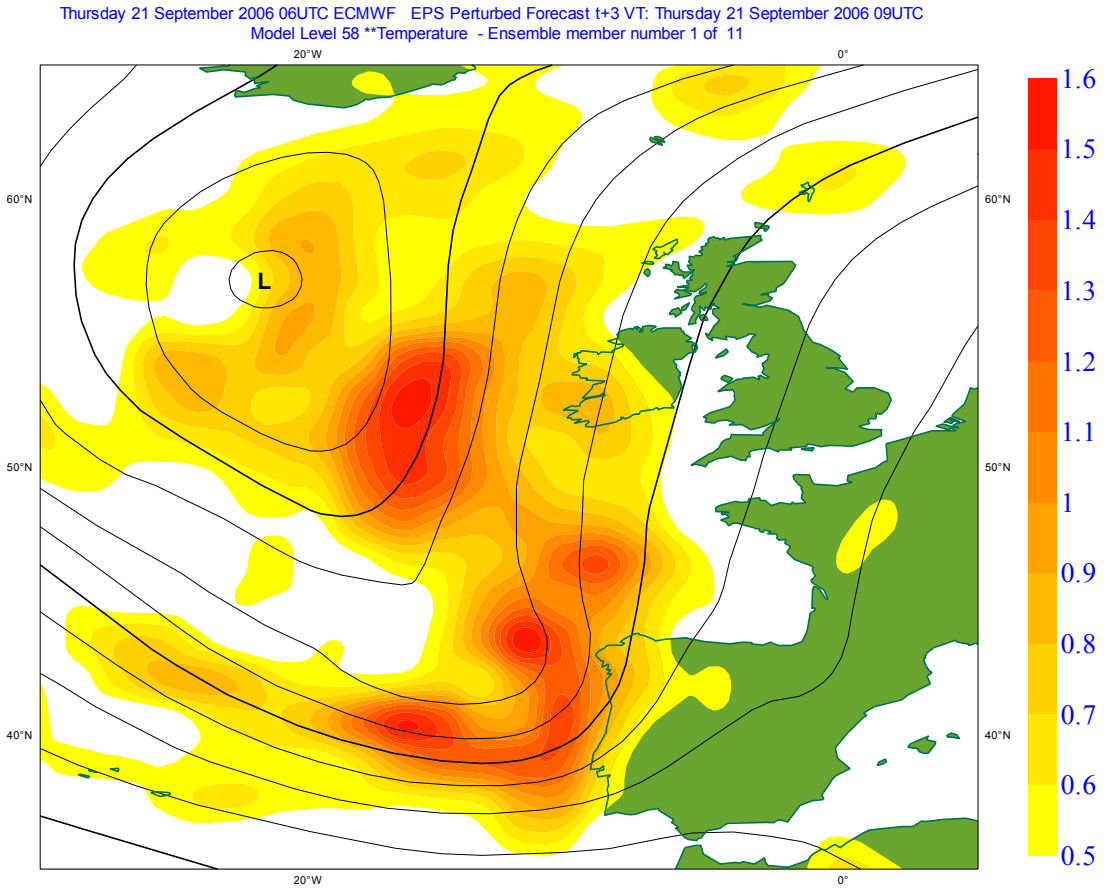

2. The ECMWF Integrated Forecasting System (IFS)

PDF(0) << 4DVAR+EDA^{25}+ORAS4^{5}
PDF(0) << ERAI+ORAS4^{5} (refc suite)
PDF(T) << HRES+ENS^{51}/S4^{51}

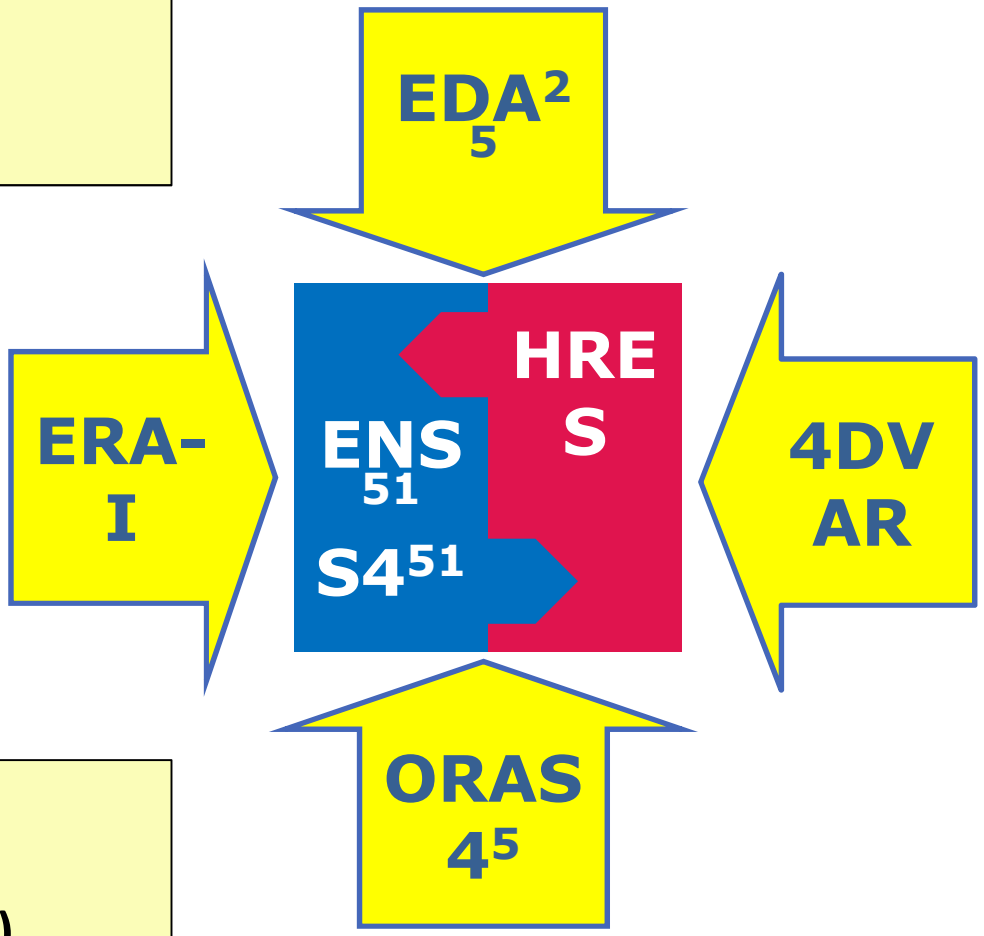

System components simulate the effect of:
- **Observation uncertainties**
- **Model uncertainties (2 stochastic schemes)**

2. EDA spread sensitivity to stochastic physics

T850 EDA spread sensitivity to model error

- NOST
- BS (back-scatter)
- SP1M (rev SPPT)
- SP1M+BS
- Jb (model error from Jb stats)
- MA5C: 5-member multi-analysis system.

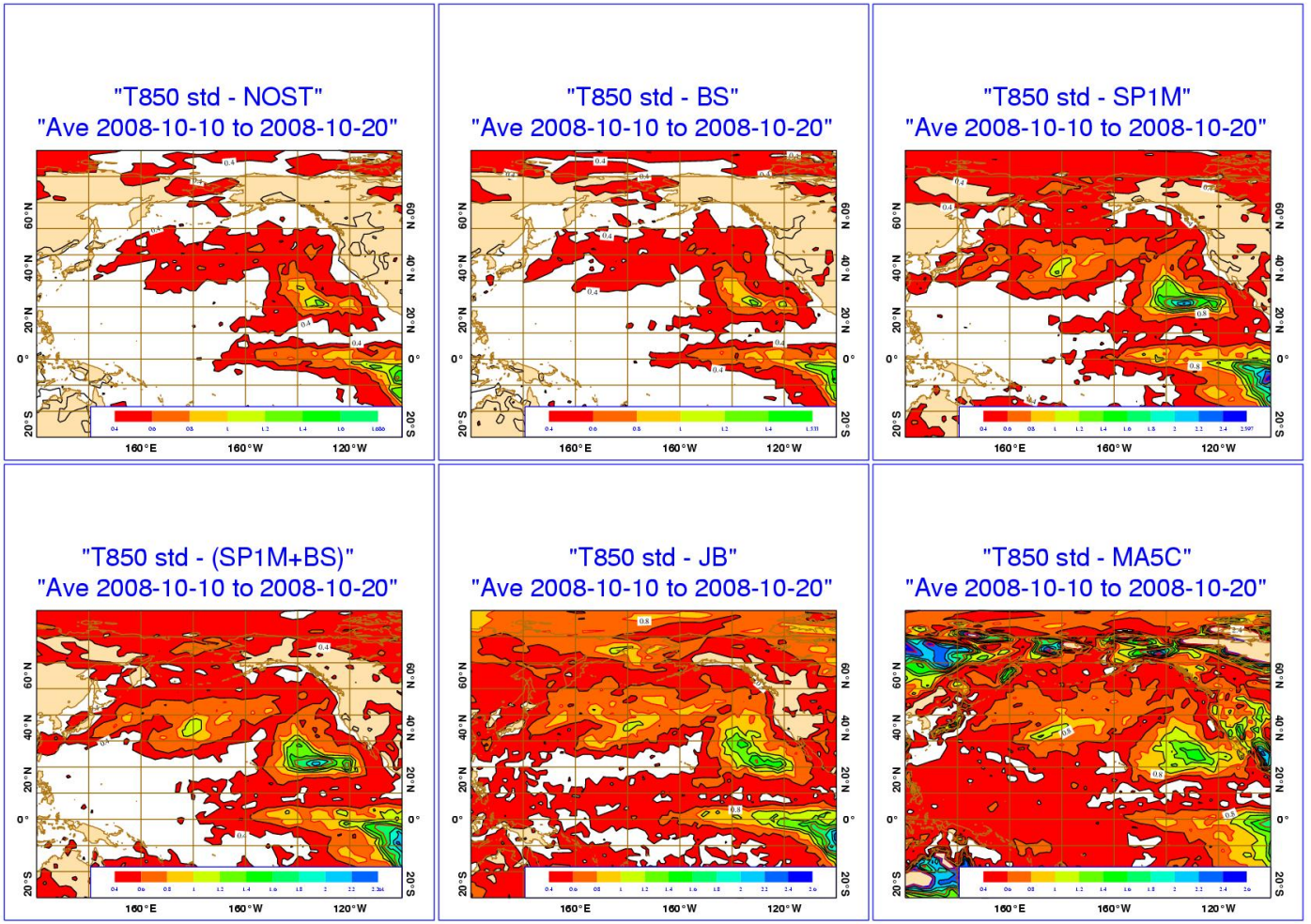

2. EDA spread sensitivity to stochastic physics

EDA spread sensitivity to model error scheme: relative impact for different variables and levels over NH.

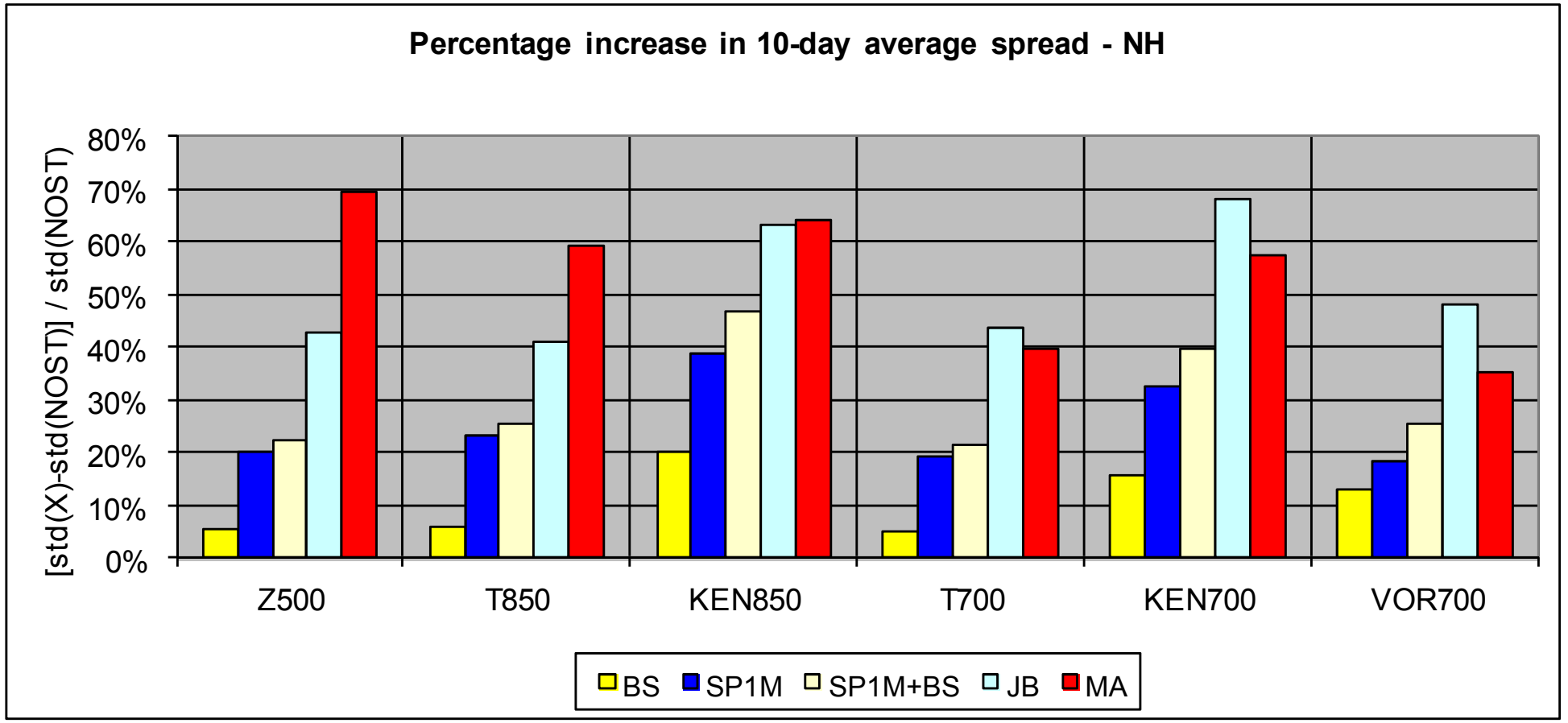

2. EDA spread as an indicator of analysis error

On the 23rd of Dec 2009 a cyclone that developed during the previous 36h in the Atlantic reached Portugal and caused lots of damages.

T799 (operational suite) and T1279 (e-suite) analyses on 21st of Dec showed larger differences in the area of storm development, and forecasts starting from these two analyses differed substantially.

Did the EDA identify the Atlantic area where the 799 and the 1279 analyses differ as an area with large spread?

2. The EDA spread as an indicator of analysis error

On the 23rd of Dec 2009 a well defined cloud head with a dry slot region ahead of the low centre can be seen in a Meteosat satellite image (left). An area of maximum radial velocity can be seen from the Doppler radar (east of Lisbon).

St Cabo Carvoeiro – Min mslp 969 hPa at 0420 UTC – Max wind gust 140 km/h at 0450 UTC

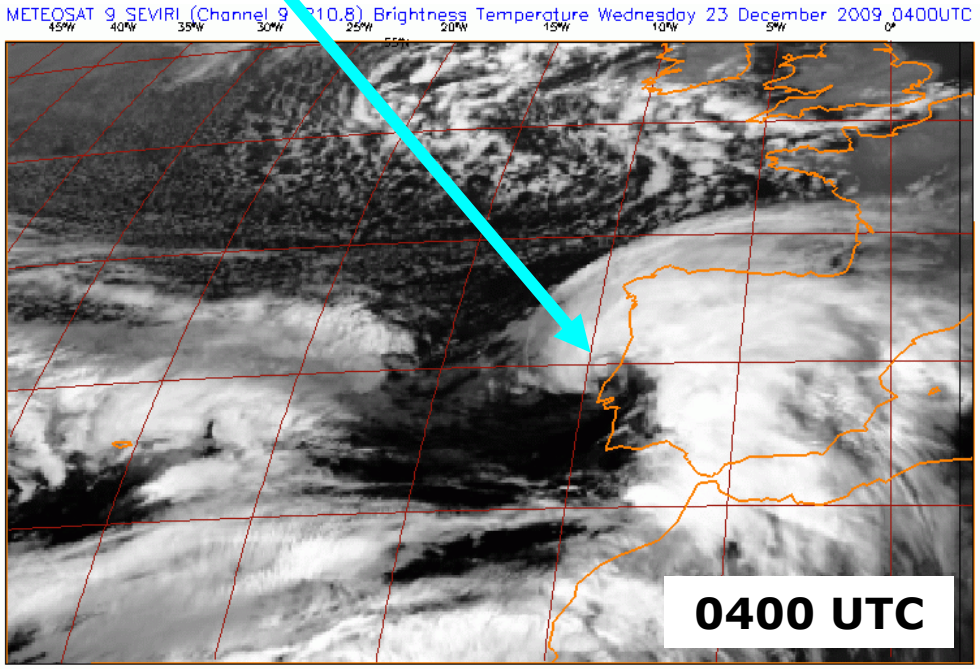

Max winds at fixed elention angle 0.1(quasi-horizontal map)

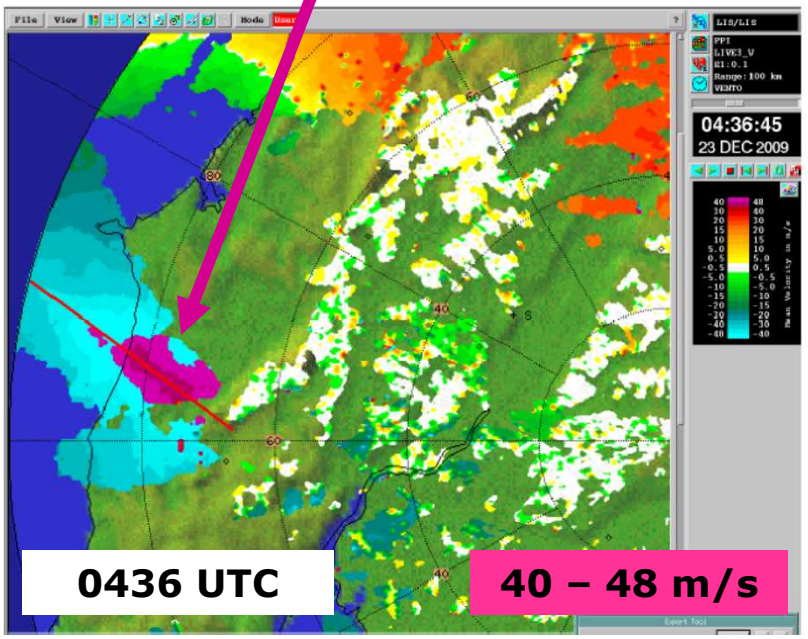

2. EDA spread as an indicator of analysis error

At that time two analysis and ensembles were running:

- O-suite: operational T799 analysis and EVO-SVINI 639v319 ENS
- E-suite: the new T1279 analysis and the EDA-SVINI 639v319 ENS

Let's compare the spread of the old (EVO-SVINI) and new (EDA-SVINI) ensembles, to assess whether the EDA-based perturbations improved the simulation of the analysis uncertainty.

2. EDA spread as an indicator of analysis error

IC 20@12:

- the top row shows the two analyses and their difference.
- the bottom row shows the std of the EVO-SVINI and the EDA-SVINI ensembles, and their difference.

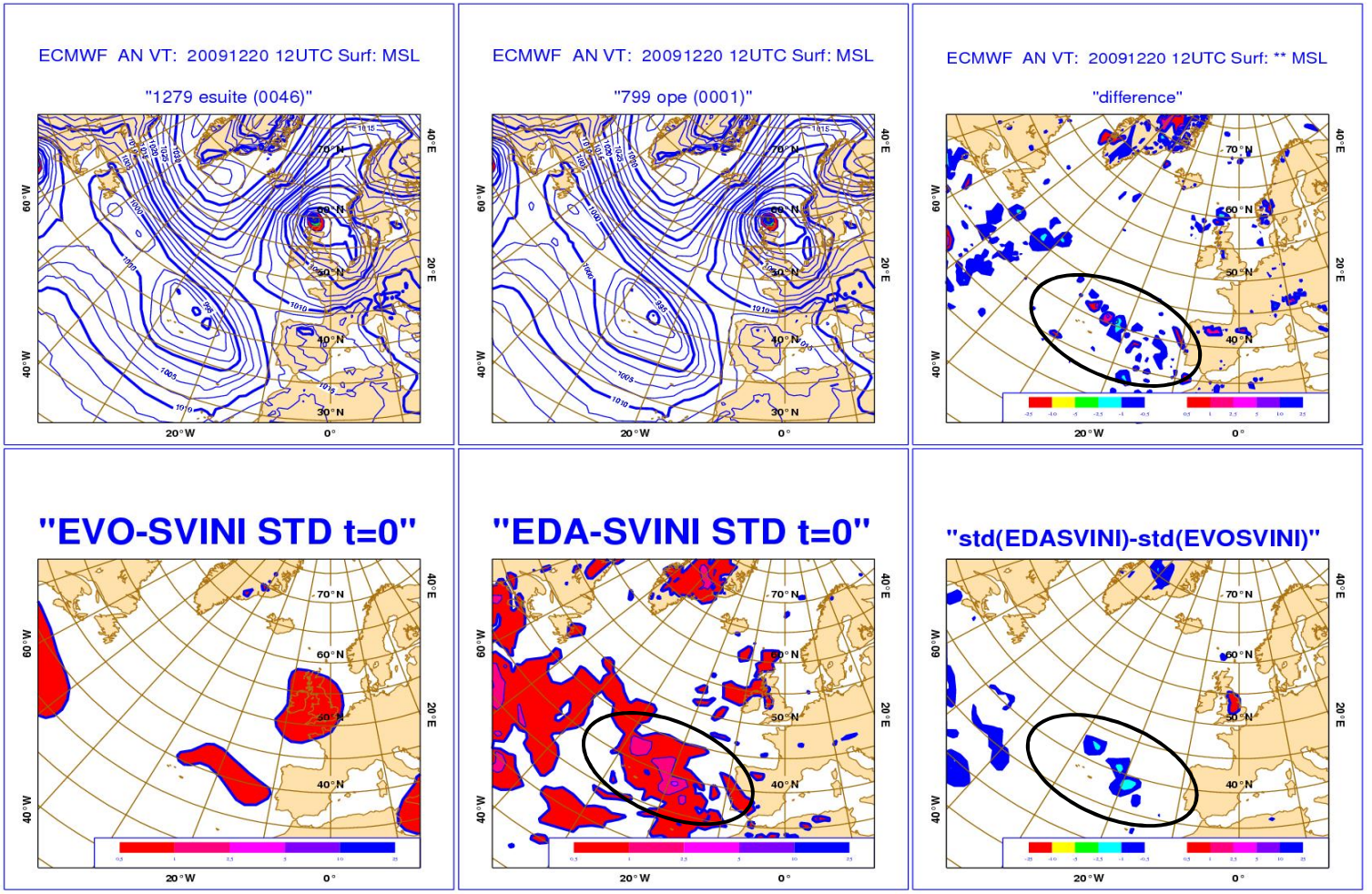

2. EDA spread as an indicator of analysis error

IC 21@12:

- the top row shows the two analysis and their difference.
- the bottom row shows the std of the EVO-SVINI and the EDA-SVINI ensembles, and their difference.

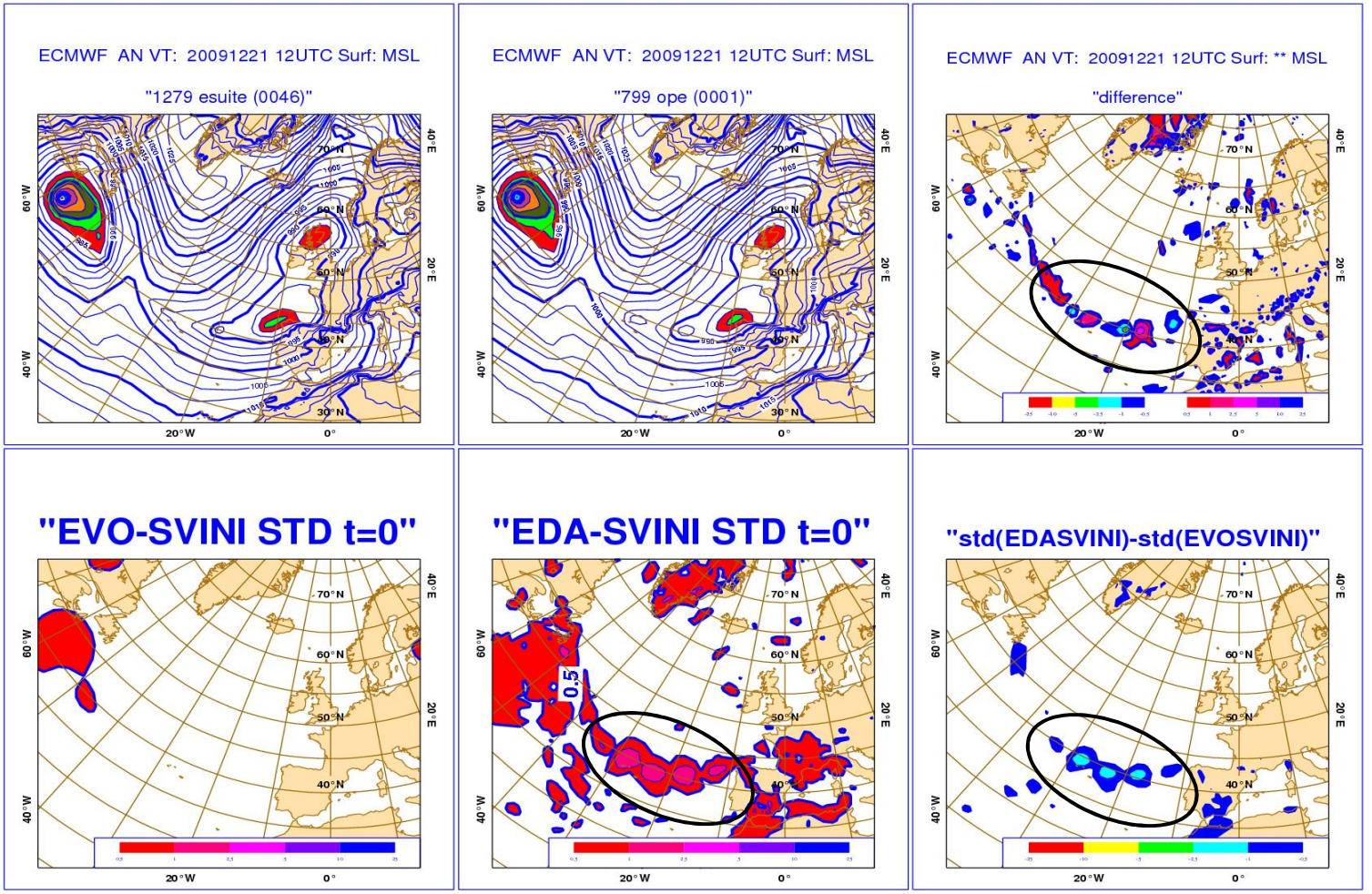

2. EDA spread as an indicator of analysis error

IC 22@12:

- the top row shows the two analyses and their difference.
- the bottom row shows the std of the EVO-SVINI and the EDA-SVINI ensembles, and their difference.

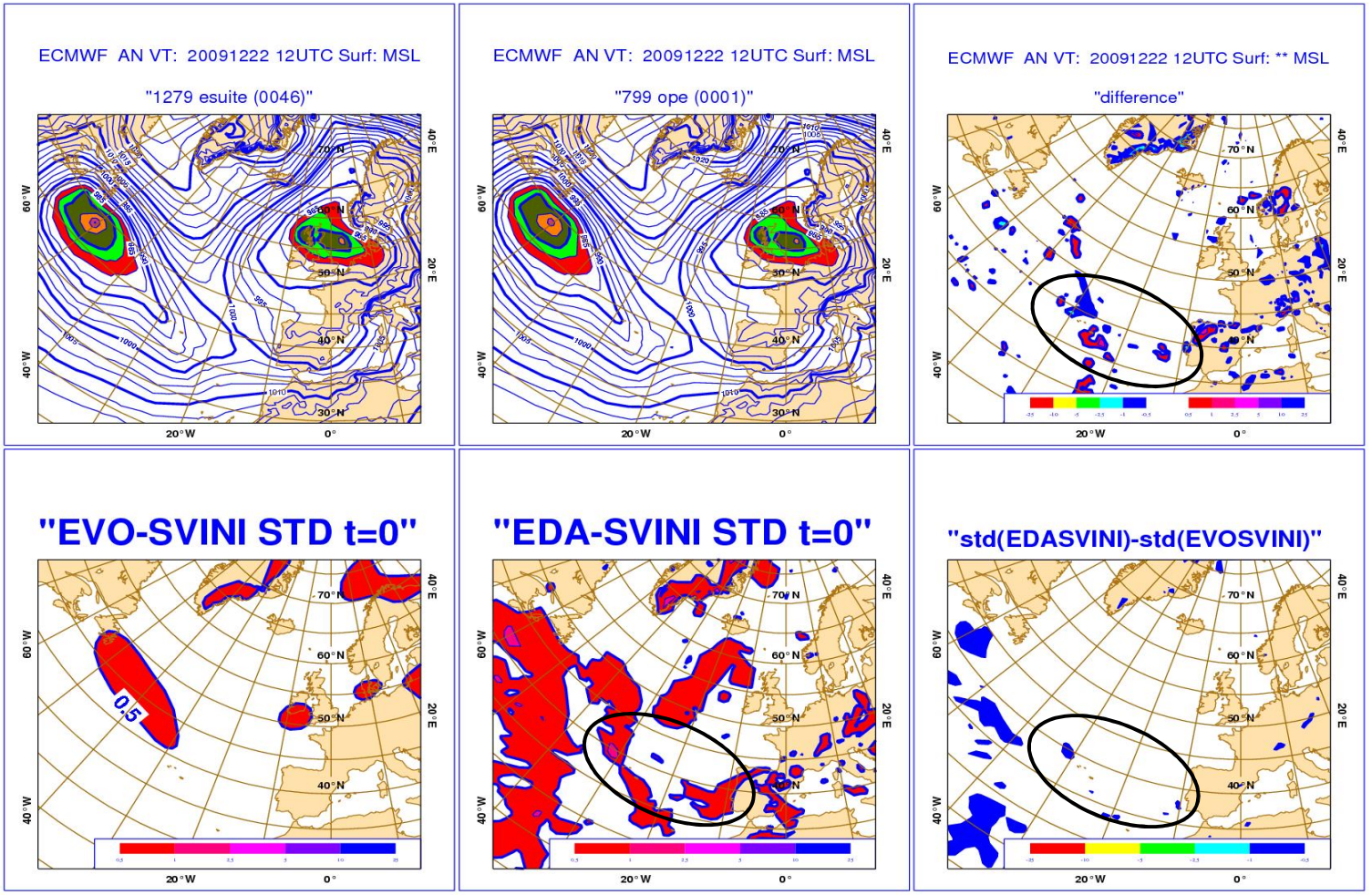

Outline

1. The original SV-based ECMWF ensemble
2. Ensemble Data Assimilation characteristics
3. The EDA-SVINI ensemble

3. The EDA-SVINI ENS

Each ensemble forecast is given by the time integration of perturbed equations

$$e_j(d,T) = e_j(d,0) + \int_0^T [A(e_j,t) + P(e_j,t) + \delta P_j(e_j,t)]dt$$

$$\delta P_j(\lambda,\phi,p) = r_j(\lambda,\phi) P_j(\lambda,\phi,p)$$

Initial perturbations are defined using 25 perturbed analyses (generated by the ECMWF Ensemble of Data Assimilations) and initial singular vectors (SVINI)

$$e_j(d,0) = e_0(d,0) + PA_j(d,0) + \sum_{area} \sum_{k=1}^{N_{SV}} [\alpha_{j,k} \cdot SV_k(d,0)]$$

$$PA_j(d,0) = [A_j(d-6h,6h) - < A_j(d-6h,6h) >_{j=1,N_{EDA}}]$$

with the 'central' (unperturbed) analysis defined by

$$e_0(d,0) = A_{T_L 1279 L137}(d,0)$$

3. The EDA-SVINI ENS

Consider the 00UTC ENS:

- EVO-SVINI ENS: the initial perturbations were generated using initial-time and evolved SVs.
- EDA-SVINI ENS: the evolved SVs are replaced by EDA-based perturbations, defined by differences between 6h forecasts from the previous-cycle EDA (blue lines).

The unperturbed (control) analysis is defined by the 6h HRES 4DVAR analysis (green box), with fg started from the previous DCDA analysis (black box).

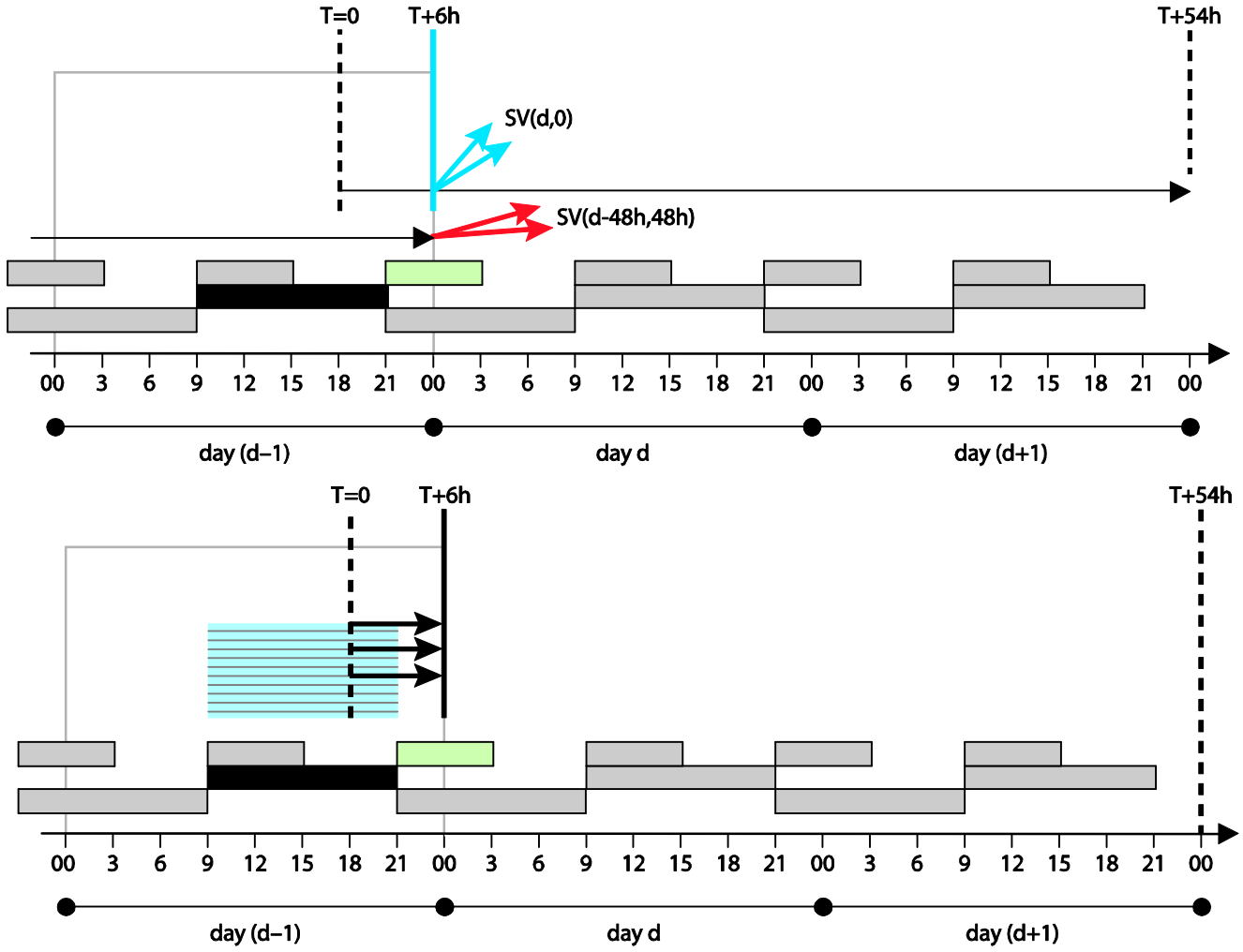

3. Ensemble experiments

What is the impact of the ENS reliability and skill of using the EDA?

- These results are based on a set of T_L399L62 ensembles (model cycle 31r2)
- The following 4 ensembles configurations are compared:
  - **SVINI**: with initial uncertainties defined by initial SVs only
  - **SVEVO-INI**: with initial uncertainties defined by evolved and initial SVs
  - **EDA**: with initial uncertainties defined by EDA-only initial perturbations
  - **EDA-SVINI**: with initial uncertainties defined by EDA- and initial SVs

3. std EDA, SVINI & EDA-SVINI - t0 (22/09/07)

EDA-only initial perturbations (left panels) are smaller in amplitudes and in scale than SVINI perturbations (middle panels), but are geographically more global.

The right panels show the effect of using both EDA and SVINI perturbations.

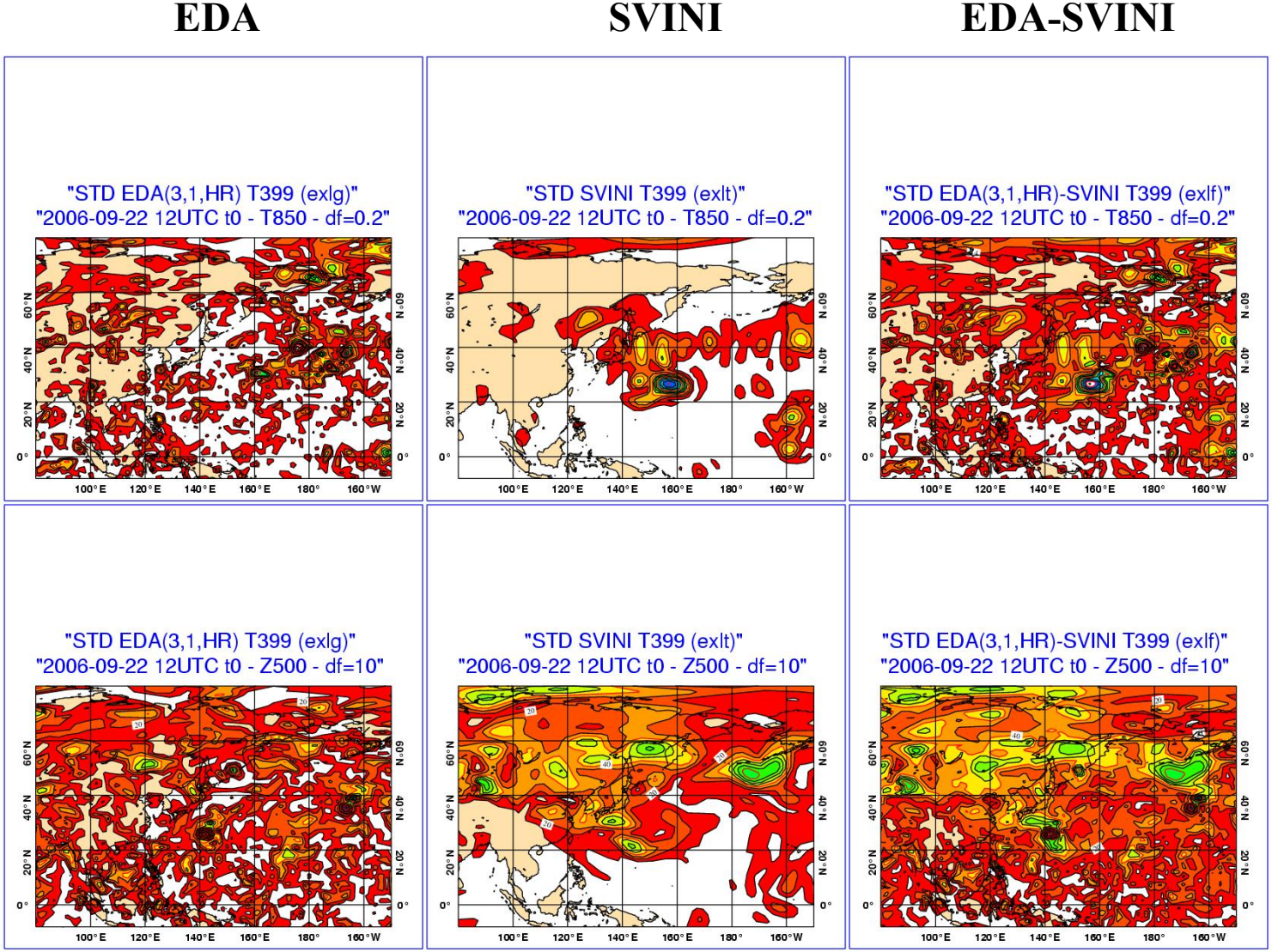

3. std EDA, SVINI & EDA-SVINI - t+12h

EDA perturbations (left panels) grow less rapidly than SVINI perturbations (middle panels).

In the combined EDA-SVINI ensemble, the SVINI component dominates the perturbations' growth.

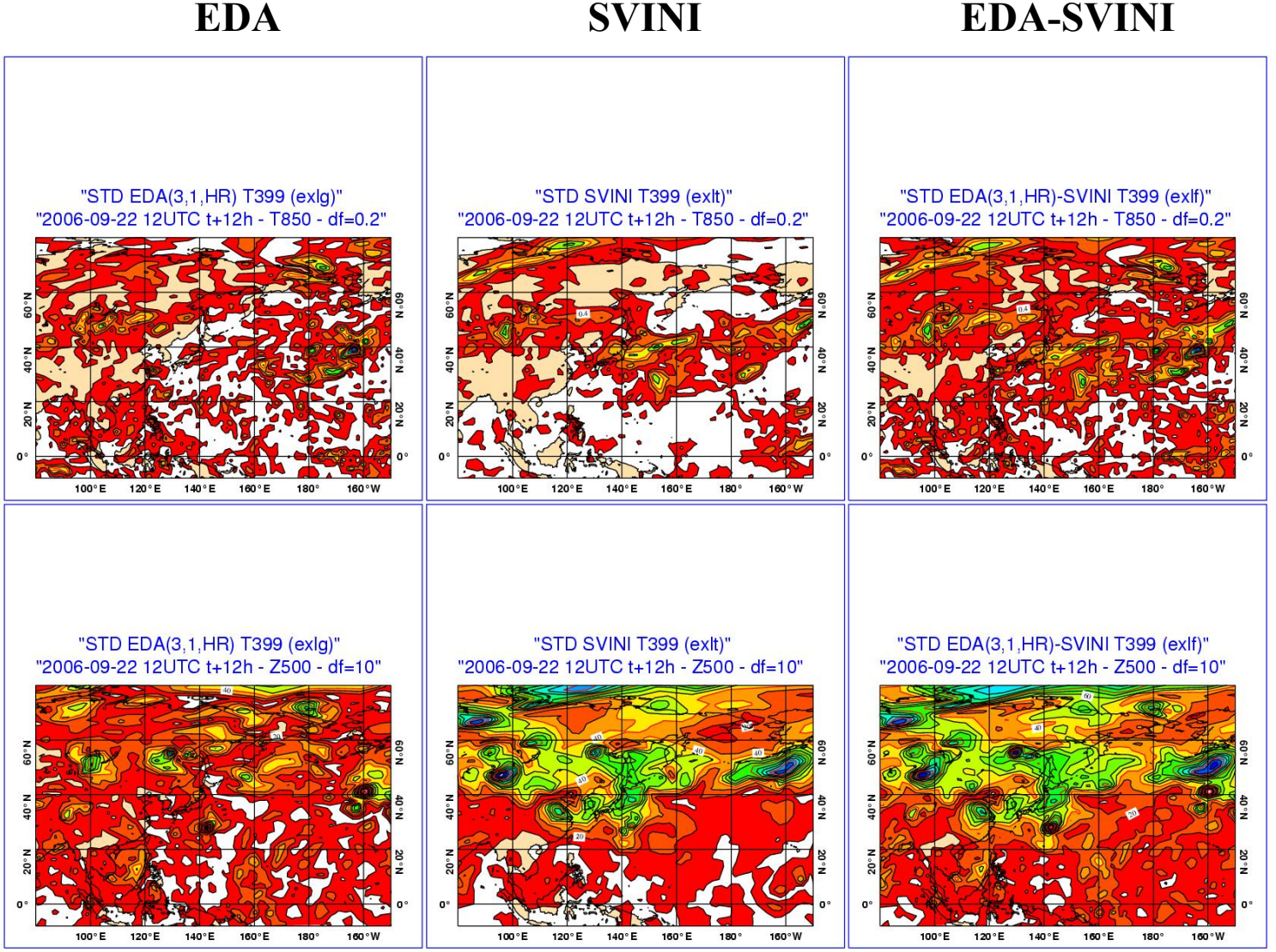

3. (MEM5-CON) SVINI ENS - 22/09/2007 t=0

At t=0, SVINI perturbations are more localized in space, and have a larger component in potential than kinetic energy. They also show a westward tilt with high, typical of baroclinically unstable structures.

T – (MEM5-CON) | **U – (MEM5-CON)**

30°N

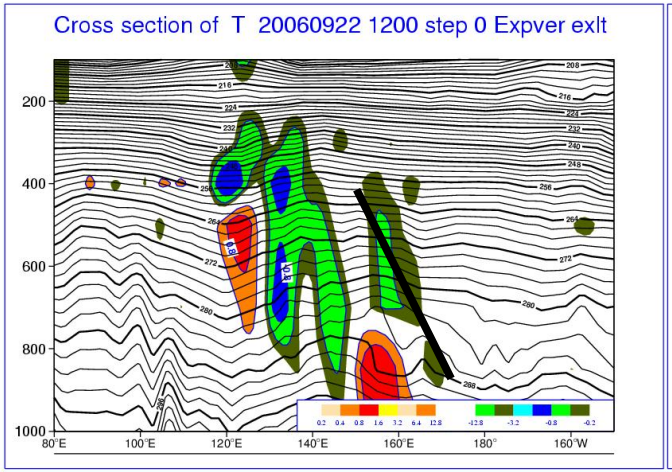

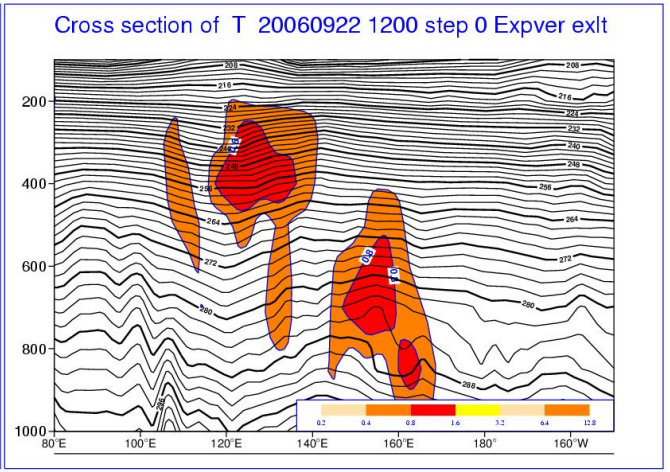

50°N

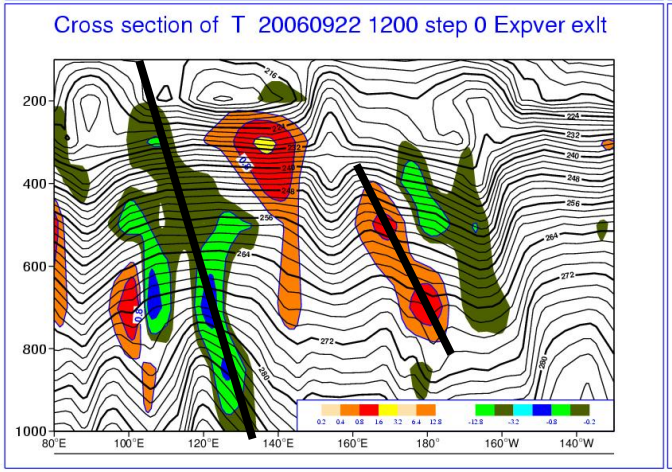

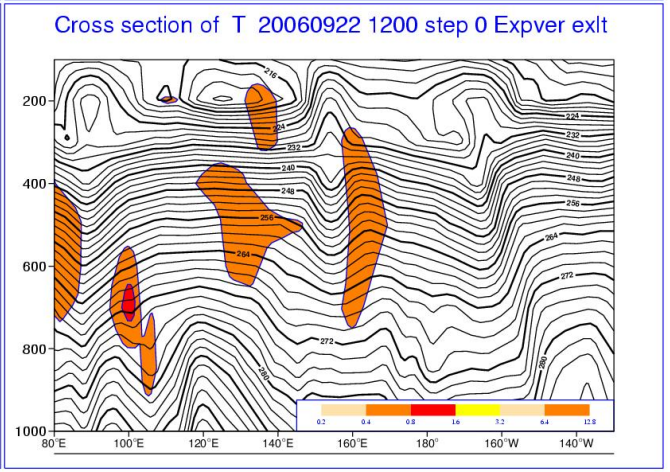

3. (MEM5-CON) EDA ENS - 22/09/2007 t=0

At t=0, EDA perturbations have a smaller scale than the SVINI perturbations, and are less localized in space. They have a similar amplitude in potential and kinetic energy. They tend to have more a barotropic than a baroclinic structure.

T – (MEM5-CON) | **U – (MEM5-CON)**

30°N

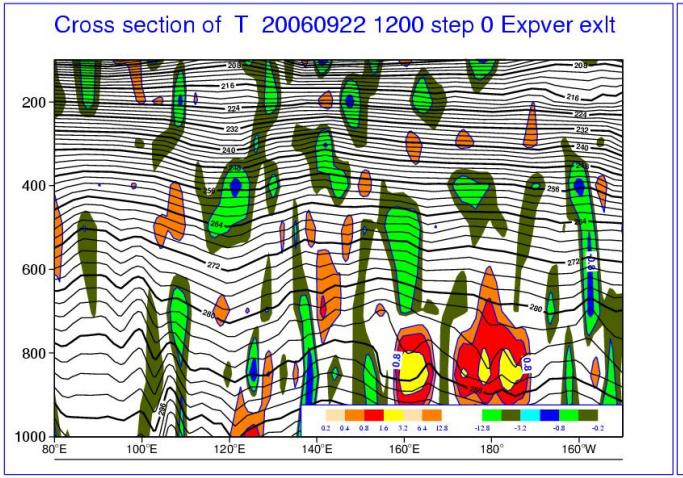

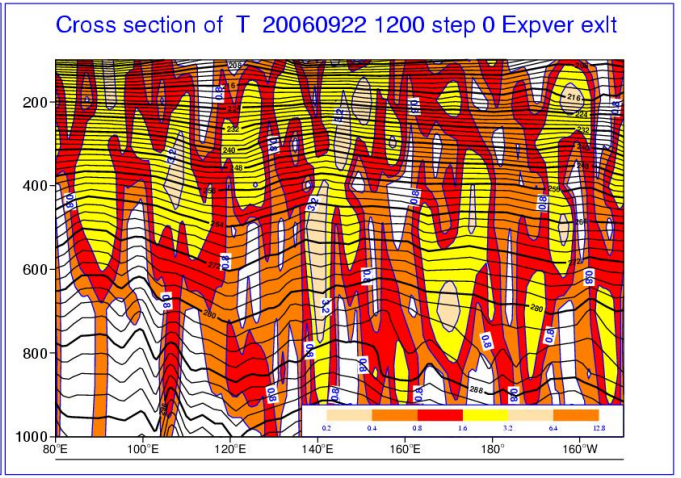

50°N

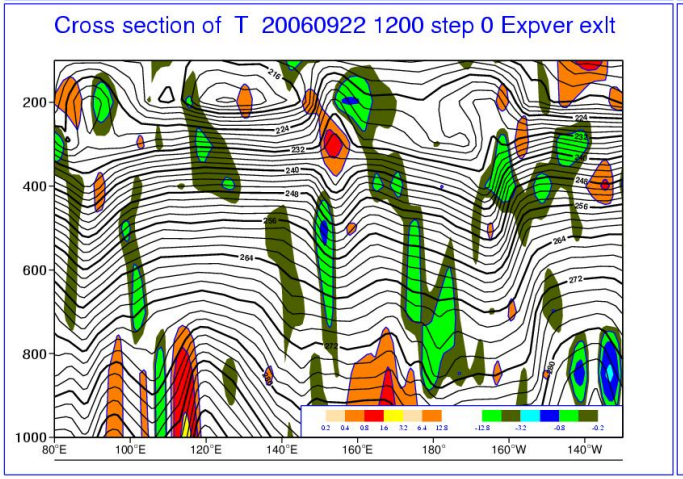

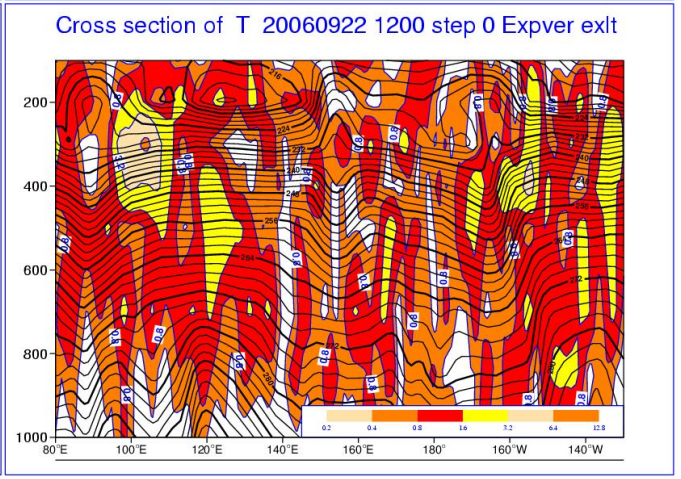

3. Spectra of EDA & SVINI ENS – NH t0

The top figure shows the squared amplitude of the SVINI (red) and EDA (blue) perturbations in terms of Z500 over NH. The bottom panel shows the same but for T850. Results have been averaged over 13 cases.

At initial time, the SVINI perturbations are confined to T42 by construction.

The EDA perturbations are larger in terms of T850.

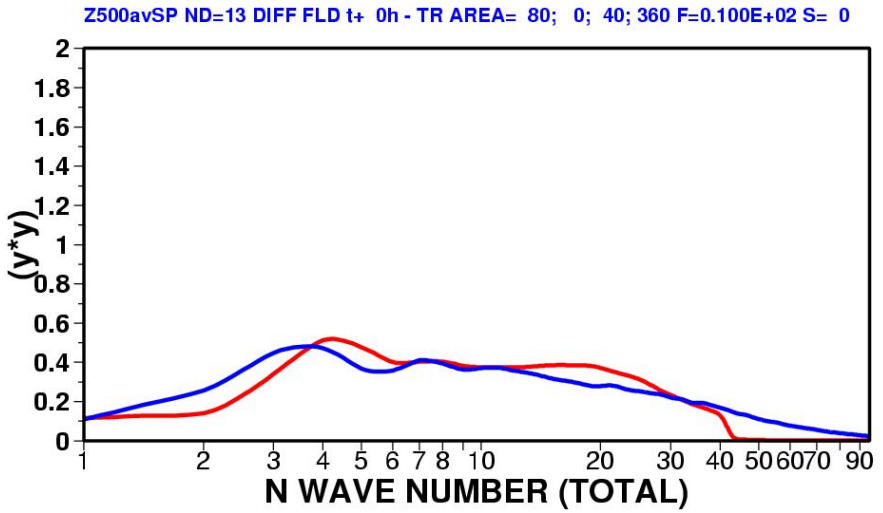

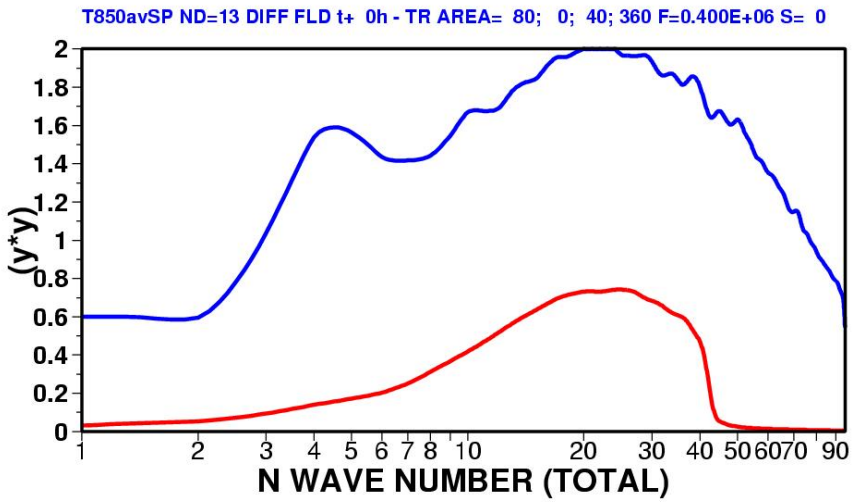

3. Spectra of EDA & SVINI ENS – NH +48h

The top figure shows the squared amplitude of the SVINI (red) and EDA (blue) perturbations in terms of Z500 over NH, and of the error of the t+48h control forecast (black). The bottom panel shows the same but for T850. Results have been averaged over 13 cases.

At t+48h, the SVINI perturbations have a larger amplitude than the EDA perturbations, especially in the wave-numbers where the SVs total energy peaks at optimisation time.

On average, the spectra of the SVINI ensemble spread is closer to the spectra of the control error.

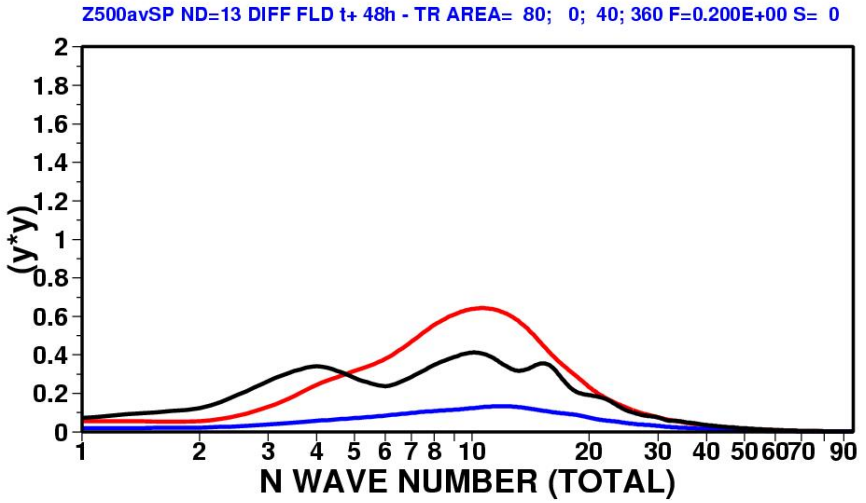

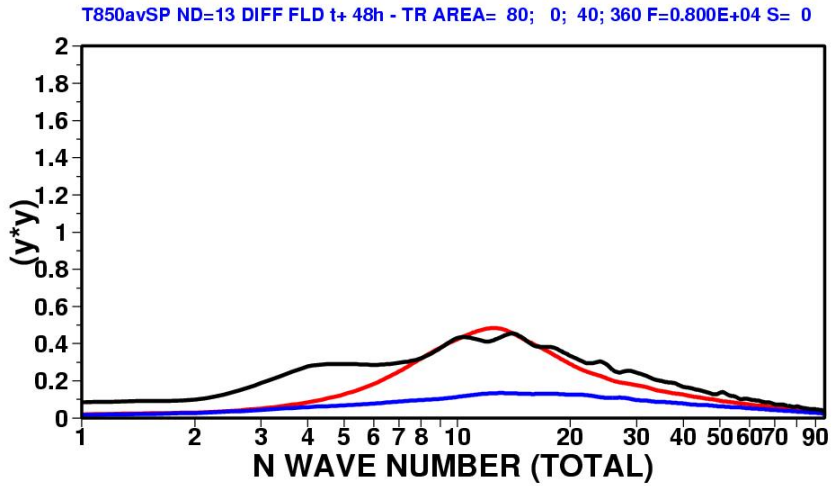

3. Spectra of EDA & SVINI ENS – NH +120h

The top figure shows the squared amplitude of the SVINI (red) and EDA (blue) perturbations in terms of Z500 over NH, and of the error of the t+120h control forecast (black). The bottom panel shows the same but for T850. Results have been averaged over 13 cases.

At t+120h, the difference in spread between the SVINI and the EDA is even more evident.

On average, the spectra of the SVINI ensemble spread is very close to the spectra of the control error.

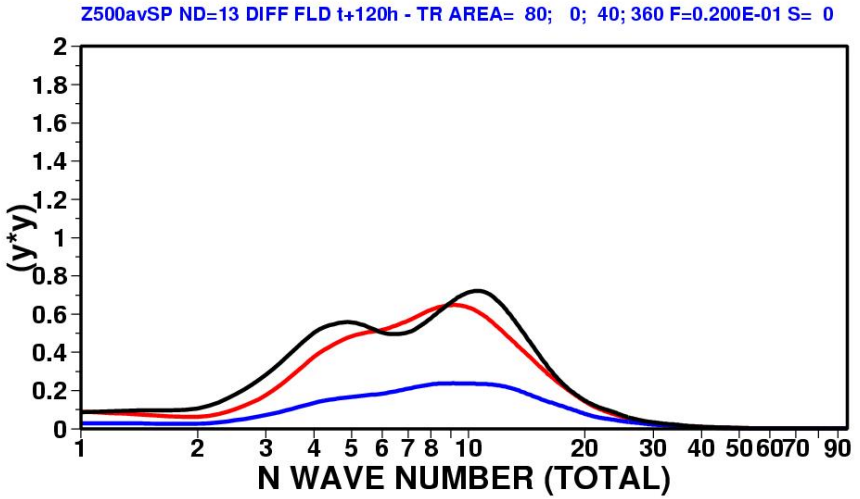

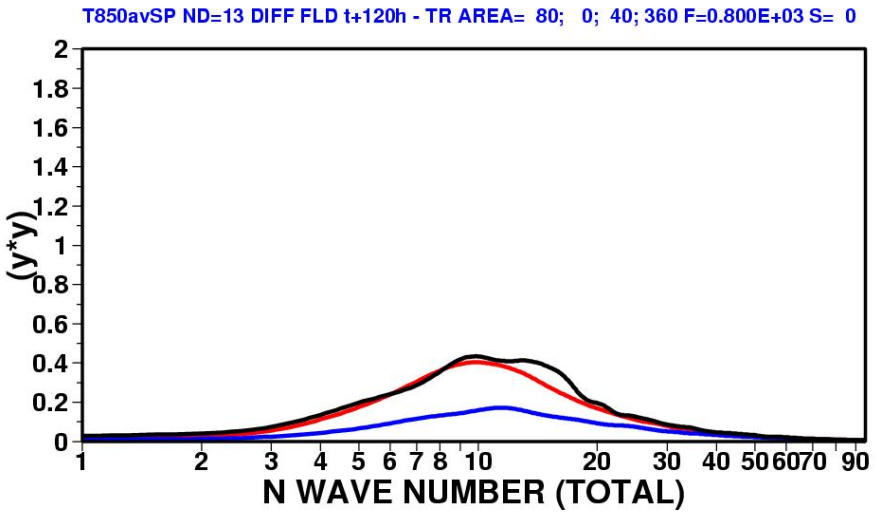

3. std/EM of EDA and SVINI ENS

Over the NH (left), the EDA ensemble have smaller spread, and a larger ensemble-mean error from forecast day 3.

Over the Tropics (right), the EDA ensemble has larger spread (in terms of T850), and this has a small positive impact on the error of the ensemble-mean, which is slightly smaller between forecast day 2 and 6.

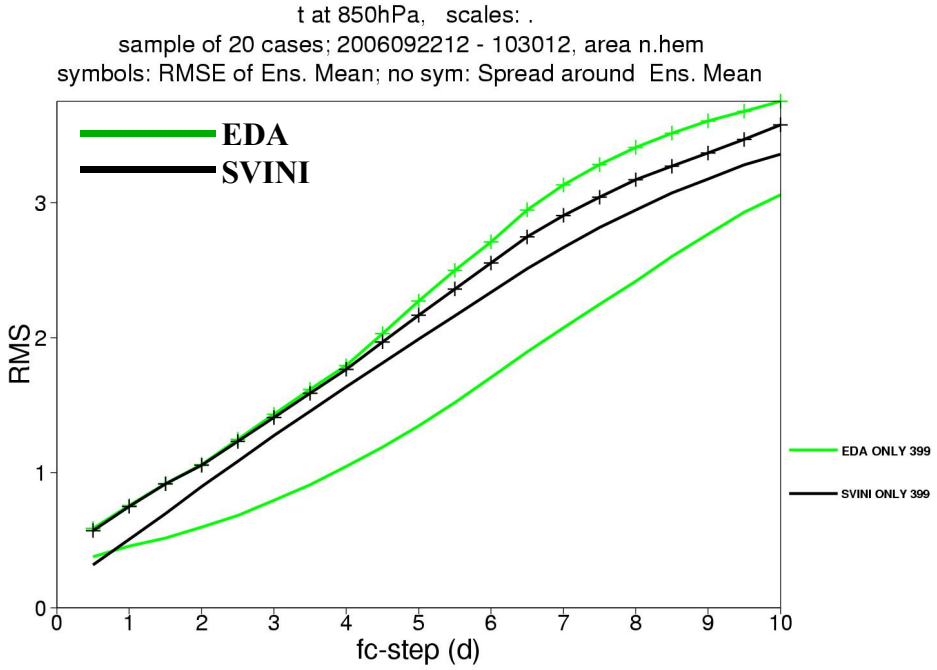

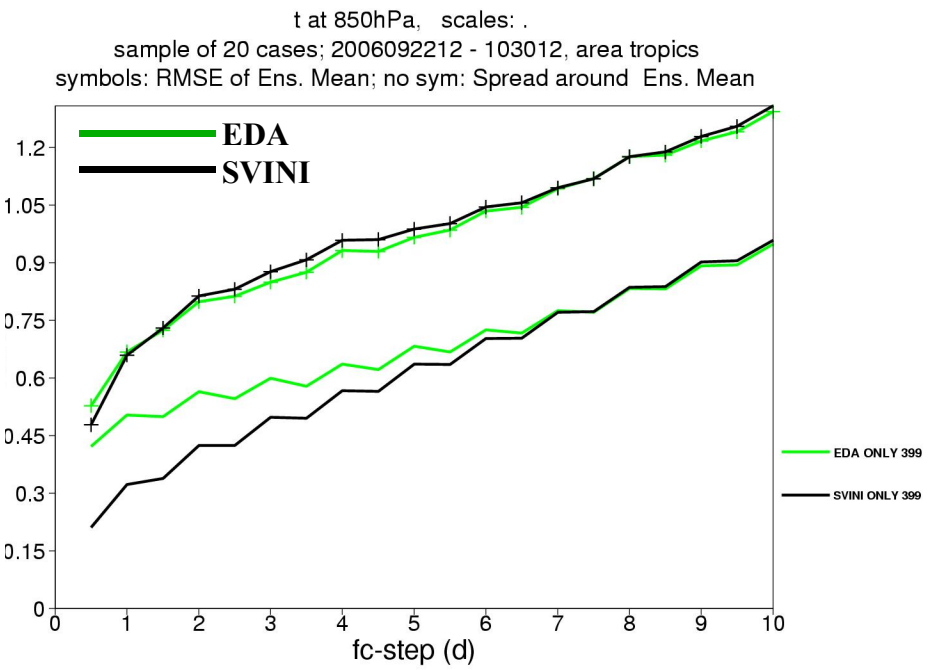

3. RPSS of EDA and SVINI ENS

Over the NH (left), the EDA ensemble has a smaller RPSS for T850 probabilistic predictions from forecast day 3, while over the tropics it has a higher RPSS from day 1 (right panel).

These results suggest that combining the ensemble of analysis and the initial singular vectors would lead to a better system.

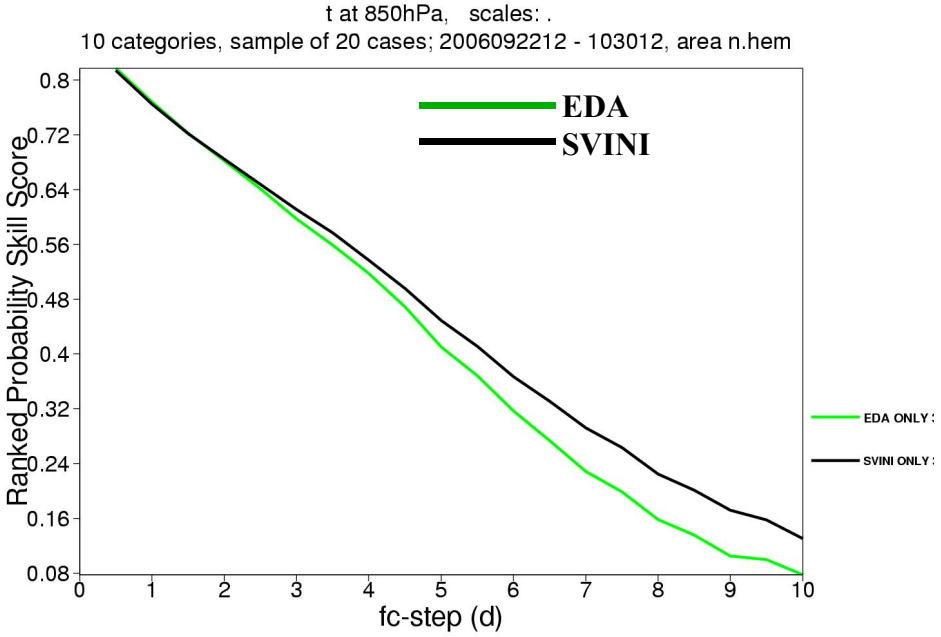

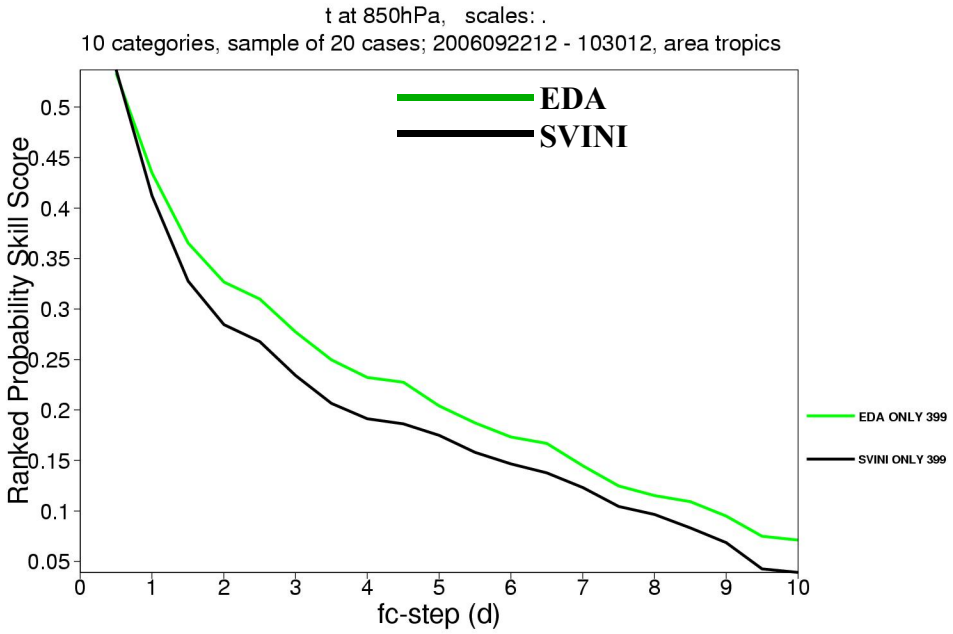

3. EDA, SVINI, EDA-SVINI & SVEVO-INI ENS

The EDA-SVINI ensemble combines the benefits of the EDA and the SV techniques. Over both the NH (left), the EDA-SVINI ensemble is only marginally better than the SVEVO-INI ensemble. But over the tropics (right), the EDA-SVINI ensemble has a higher RPSS. Note that the combination of EDA- and SVINI-based perturbations leads to an ensemble that outperforms one based on EDA-based perturbations only.

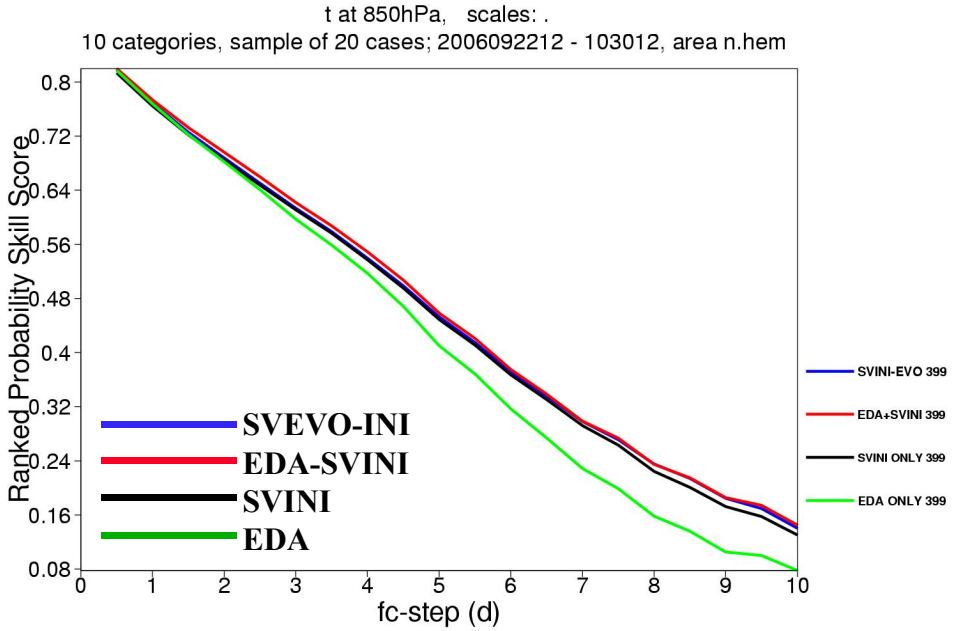

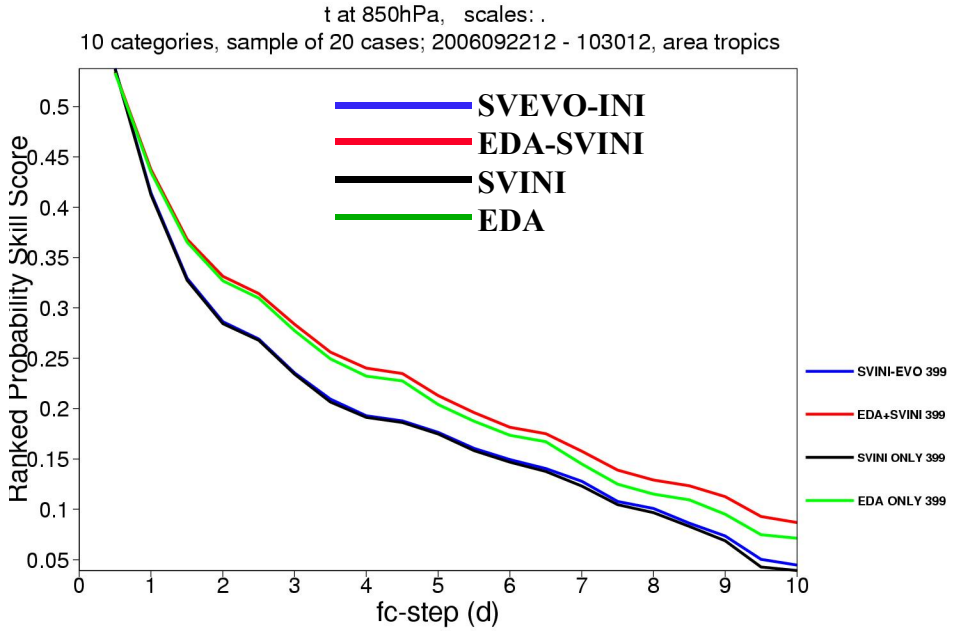

Conclusions

- SV- and EDA-based perturbations have different characteristics:
  - Geographically, EDA-based perturbations are less localized. In particular, they have a larger amplitude over the tropics.
  - Spectrally, EDA perturbations are smaller in scale.
  - Vertically, EDA-perturbations are more barotropic than SV-based perturbations, while these latter show westward tilt with height typical of baroclinically unstable structures.
  - At initial time, SV-based perturbations have a larger amplitude in potential than kinetic energy, while EDA-based perturbations have a similar amplitude in potential and kinetic energy.
  - EDA perturbations grow less rapidly.

- An EDA-based ensemble severely underestimate the ensemble spread
- More reliable and accurate forecasts are obtained with a combination of EDA- and SV-based perturbations (operational since Jun 2010).

Acknowledgements

The success of the ECMWF ensemble is the result of the continuous work of ECMWF staff, consultants and visitors who had continuously improved the ECMWF model, analysis, diagnostic and technical systems, and of very successful collaborations with its member states and other international institutions. The work of all contributors is acknowledged.

Bibliography

On the ECMWF Ensemble Prediction System

- Buizza, R., & Hollingsworth, A., 2002: Storm prediction over Europe using the ECMWF Ensemble Prediction System. *Meteorol. Appl.*, **9**, 1-17.
- Buizza, R., Bidlot, J.-R., Wedi, N., Fuentes, M., Hamrud, M., Holt, G., & Vitart, F., 2007: The new ECMWF VAREPS. *Q. J. Roy. Meteorol. Soc.*, **133**, 681-695 (also EC TM 499).
- Buizza, R., 2008: Comparison of a 51-member low-resolution (TL399L62) ensemble with a 6-member high-resolution (TL799L91) lagged-forecast ensemble. *Mon. Wea. Rev.*, **136**, 3343-3362 (also EC TM 559).
- Buizza, R., Leutbecher, M., & Isaksen, L., 2008: Potential use of an ensemble of analyses in the ECMWF Ensemble Prediction System. *Q. J. R. Meteorol. Soc.*, **134**, 2051-2066.
- Buizza, R., 2010: The Value of a Variable Resolution Approach to Numerical Weather Prediction. *Mon. Wea. Rev.*, **138**, 1026-1042.
- Leutbecher, M. 2005: On ensemble prediction using singular vectors started from forecasts. ECMWF TM 462, pp 11.
- Leutbecher, M. & T.N. Palmer, 2008: Ensemble forecasting. *J. Comp. Phys.*, **227**, 3515-3539 (also EC TM 514).

Bibliography

- Molteni, F., Buizza, R., Palmer, T. N., & Petroliagis, T., 1996: The new ECMWF ensemble prediction system: methodology and validation. *Q. J. R. Meteorol. Soc.*, **122**, 73-119.
- Palmer, T N, Buizza, R., Leutbecher, M., Hagedorn, R., Jung, T., Rodwell, M, Virat, F., Berner, J., Hagel, E., Lawrence, A., Pappenberger, F., Park, Y.-Y., van Bremen, L., Gilmour, I., & Smith, L., 2007: The ECMWF Ensemble Prediction System: recent and on-going developments. A paper presented at the 36th Session of the ECMWF Scientific Advisory Committee (also EC TM 540).
- Palmer, T. N., Buizza, R., Doblas-Reyes, F., Jung, T., Leutbecher, M., Shutts, G. J., Steinheimer M., & Weisheimer, A., 2009: Stochastic parametrization and model uncertainty. ECMWF RD TM 598, Shinfield Park, Reading RG2-9AX, UK, pp. 42.
- Vitart, F., Buizza, R., Alonso Balmaseda, M., Balsamo, G., Bidlot, J. R., Bonet, A., Fuentes, M., Hofstadler, A., Molteni, F., & Palmer, T. N., 2008: The new VAREPS-monthly forecasting system: a first step towards seamless prediction. *Q. J. Roy. Meteorol. Soc.*, **134**, 1789-1799.
- Vitart, F., & Molteni, F., 2009: Simulation of the MJO and its teleconnections in an ensemble of 46-day EPS hindcasts. ECMWF RD TM 597, Shinfield Park, Reading RG2-9AX, UK, pp. 60.
- Zsoter, E., Buizza, R., & Richardson, D., 2009: 'Jumpiness' of the ECMWF and UK Met Office EPS control and ensemble-mean forecasts'. *Mon. Wea. Rev.*, 137, 3823-3836.

Bibliography

On different approaches to ensemble prediction

- Bourke, W., Buizza, R., & Naughton, M., 2004: Performance of the ECMWF and the BoM Ensemble Systems in the Southern Hemisphere. *Mon. Wea. Rev.*, **132**, 2338-2357.
- Buizza, R, Houtekamer, P L, Toth, Z, Pellerin, G, Wei, M, & Zhu, Y, 2005: A comparison of the ECMWF, MSC and NCEP Ensemble Prediction Systems. *Mon. Wea. Rev.*, **133**, 1076-1097.
- Harrison, M, Palmer, T N, Richardson, D, & Buizza, R, 1999: Analysis and model dependencies in medium-range ensembles: two transplant case studies. *Q. J. R. Meteorol. Soc.*, **126**, 2487-2515.
- Hagedorn, R., Buizza, R., Hamill, M. T., Leutbecher, M., & Palmer, T. N., 2010: Comparing TIGGE multi-model forecasts with re-forecast calibrated ECMWF ensemble forecasts. *Mon. Wea. Rev.*, submitted.
- Majumdar, S, Bishop, C, Buizza, R, & Gelaro, R, 2002: A comparison of PSU-NCEP Ensemble Transform Kalman Filter targeting guidance with ECMWF and NRL Singular Vector guidance. Q*. J. R. Meteorol. Soc*., **128**, 2527-2549.

On ensemble data assimilation and prediction

- Buizza, R., Leutbecher, M., & Isaksen, L., 2008: Potential use of an ensemble of analyses in the ECMWF ensemble prediction system. *Q. J. R. Meteorol. Soc.*, **134**, 2051-2066.
- Leutbecher, M., Buizza, R., & Isaksen, L., 2008: Ensemble forecasting and flow-dependent estimates of initial uncertainty. Proceedings of the ECMWF Workshop on Flow dependent aspects of data-assimilation, 11-13 June 2007, pp. 185-201 (available from ECMWF, Shinfield Park, Reading RG2-9AX).

Bibliography

On SVs and targeting adaptive observations:

- Buizza, R., & Montani, A., 1999: Targeting observations using singular vectors. *J. Atmos. Sci.*, **56**, 2965-2985 (also EC TM 286).
- Buizza, R., Cardinali, C., Kelly, G., & Thepaut, J.-N., 2007: The value of targeted observations - Part II: the value of observations taken in singular vectors-based target areas. *Q. J. R. Meteorol. Soc*., **133**, 1817-1832 (also EC TM 512).
- Cardinali, C., Buizza, R., Kelly, G., Shapiro, M., & Thepaut, J.-N., 2007: The value of observations - Part III: influence of weather regimes on targeting. *Q. J. R. Meteorol. Soc.*, **133**, 1833-1842 (also EC TM 513).
- Gelaro, R., Buizza, R., Palmer, T. N., & Klinker, E., 1998: Sensitivity analysis of forecast errors and the construction of optimal perturbations using singular vectors. *J. Atmos. Sci.*, **55**, 6, 1012-1037.
- Kelly, G., Thepaut, J.-N., Buizza, R., & Cardinali, C., 2007: The value of observations - Part I: data denial experiments for the Atlantic and the Pacific. *Q. J. R. Meteorol. Soc.*, **133**, 1803-1815 (also EC TM 511).
- Majumdar, S J, Aberson, S D, Bishop, C H, Buizza, R, Peng, M, & Reynolds, C, 2006: A comparison of adaptive observing guidance for Atlantic tropical cyclones. *Mon. Wea. Rev*., **134**, 2354-2372 (also EC TM 482).
- Palmer, T. N., Gelaro, R., Barkmeijer, J., & Buizza, R., 1998: Singular vectors, metrics, and adaptive observations. *J. Atmos. Sci.*, **55**, 6, 633-653.
- Reynolds, C, Peng, M, Majumdar, S J, Aberson, S D, Bishop, C H, & Buizza, R, 2007: Interpretation of adaptive observing guidance for Atlantic tropical cyclones. *Mon. Wea. Rev.,* **135**, 4006-4029.

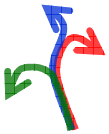

… extra material …

2. The assimilation problem

Denote by x the atmospheric state, $M(x)$ the (non-linear) model, x_b a first-guess (background) state, $H(x)$ the observation operator, ε the error fields.

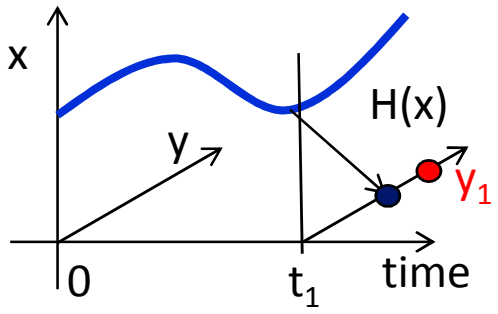

$$\frac{\partial x}{\partial t} = M(x) + \varepsilon_m$$

$$x(0) = x_b(0) + \varepsilon_b$$

$$y_j = H_j(x) + \varepsilon_{o,j}$$

Assume that the model, background and observations errors are independent and have probability density functions $P_m(\varepsilon_m, t)$, $P_b(\varepsilon_b, t)$, $P_o(\varepsilon_o, t)$.

This assumption (of independence) means that the total probability density function can be written as the product of the three:

$$P = P_m P_b P_o = \exp(\log P_m + \log P_b + \log P_o)$$

The optimal analysis x_a is the state for which the total pdf P is maximum.

(Adapted from E. Holm, 2008: Lecture notes on assimilation algorithms, ECMWF)

2. The assimilation problem

Finding the state *x(0)* for which the total pdf *P*

$$P = P_m P_b P_o = \exp(\log P_m + \log P_b + \log P_o)$$

is maximum is equivalent to finding the state *x(0)* for which the negative of the exponent of *P* has a minimum

$$\min J = \min(-\log P_m - \log P_b - \log P_o) = \min(J_m + J_b + J_o)$$

Compared to the background (blue line), following the assimilation of the observation y_1 at time t_1, the new forecast trajectory starting from x(0) goes closer to y1.

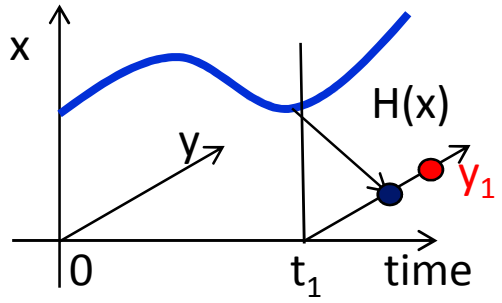

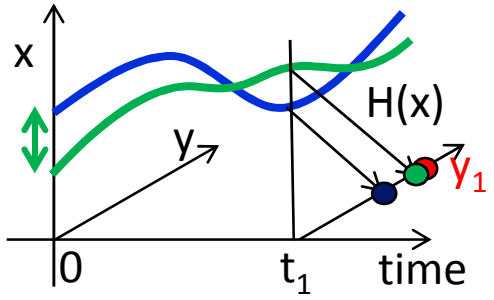

(Adapted from E. Holm, 2008: Lecture notes on assimilation algorithms, ECMWF)

2. The assimilation problem

Example. Suppose that the model error can be neglected ($\boldsymbol{\varepsilon_m}$=0) and that the observation and model errors can be modelled by a Gaussian distribution

$$P_b = \frac{1}{\sqrt{2\pi \left|\overline{\overline{B}}\right|}} e^{-\frac{1}{2}\vec{\varepsilon}_b^{\,T} \overline{\overline{B}}^{-1} \vec{\varepsilon}_b}$$

$$\vec{\varepsilon}_b = \vec{x} - \vec{x}_b$$

$$P_o = \frac{1}{\sqrt{2\pi \left|\overline{\overline{R}}\right|}} e^{-\frac{1}{2}\vec{\varepsilon}_o^{\,T} \overline{\overline{R}}^{-1} \vec{\varepsilon}_o}$$

$$\vec{\varepsilon}_o = \vec{y} - \overrightarrow{H}(\vec{x})$$

$$2J = (\vec{x} - \vec{x}_b)^T \overline{\overline{B}}^{-1} (\vec{x} - \vec{x}_b) + (\vec{y} - \overrightarrow{H}(\vec{x}))^T \overline{\overline{R}}^{-1} (\vec{y} - \overrightarrow{H}(\vec{x}))$$

The cost function is:

The analysis state x_a, is the state x that minimizes J:

$$\overline{\overline{B}}^{-1} (\vec{x}_a - \vec{x}_b) + \overrightarrow{H}(\vec{x}_a)^T \overline{\overline{R}}^{-1} (\vec{y} - \overrightarrow{H}(\vec{x}_a)) = 0$$

(Adapted from E. Holm, 2008: Lecture notes on assimilation algorithms, ECMWF)

2. The assimilation problem

Now let's approximate *H(x)* using its linear approximation *H*, and its adjoint $H(x)^T$ by the adjoint of its linear approximation H^T:

$$\vec{H}(\vec{x}_a) = \vec{H}(\vec{x}_b + \vec{x}_a - \vec{x}_b) = \vec{H}(\vec{x}_b) + \bar{\bar{H}}(\vec{x}_a - \vec{x}_b)$$

Then the linearized equation becomes:

$$\bar{\bar{B}}^{-1}(\vec{x}_a - \vec{x}_b) + \bar{\bar{H}}^T \bar{\bar{R}}^{-1}(\vec{y} - \vec{H}(\vec{x}_b) - \bar{\bar{H}}(\vec{x}_a - \vec{x}_b)) = 0$$

The solution is:

observation error covariance

$$\vec{x}_a = \vec{x}_b + \bar{\bar{B}}\bar{\bar{H}}^T(\bar{\bar{H}}\bar{\bar{B}}\bar{\bar{H}}^T + \bar{\bar{R}})^{-1}(\vec{y} - \vec{H}(\vec{x}_b))$$

background error covariance in observation space

(Adapted from E. Holm, 2008: Lecture notes on assimilation algorithms, ECMWF)

2. EDA spread sensitivity to stochastic physics

EDA spread sensitivity to model error scheme: relative impact for different variables and levels over the tropics.

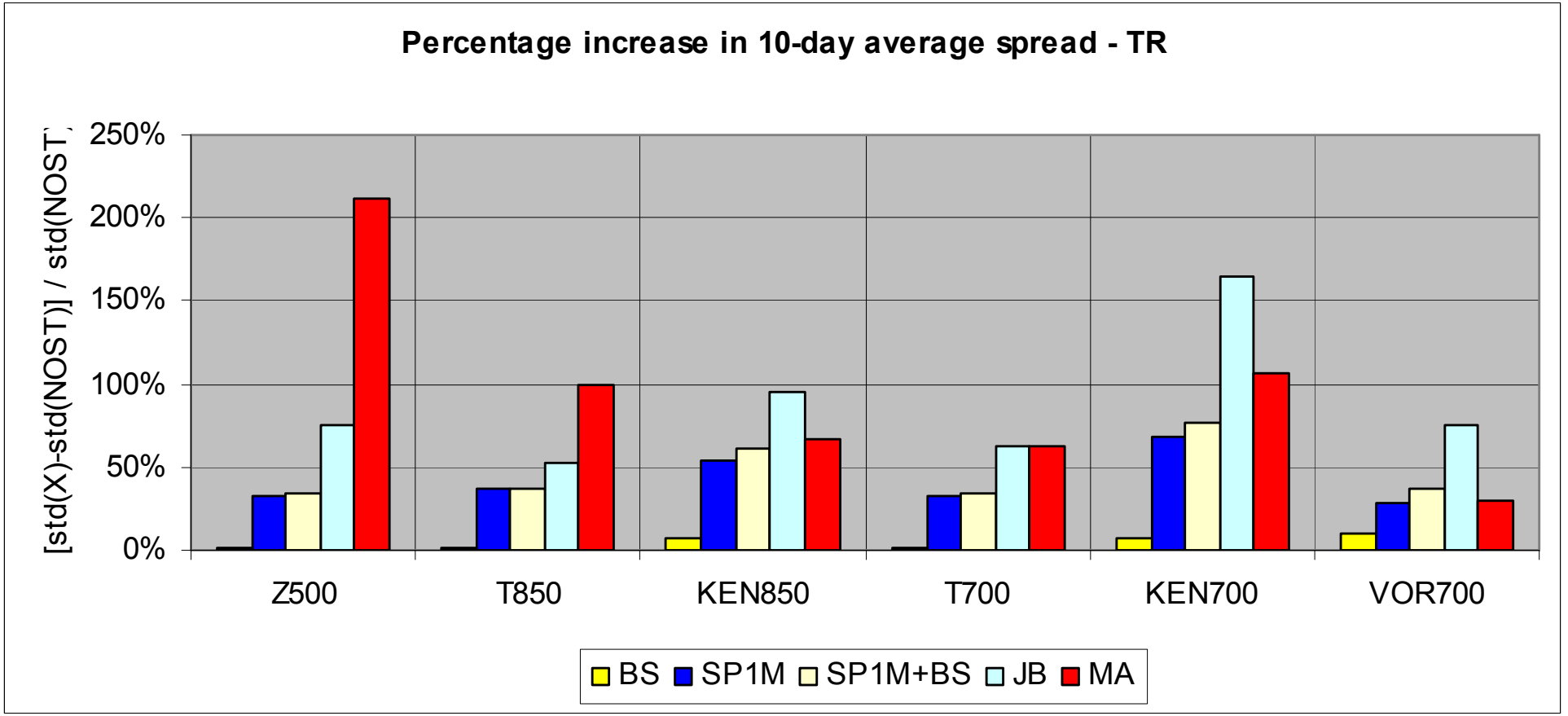

2. EDA spread as an indicator of analysis error

The tropics is the region where the old and the new ensembles differ mostly.

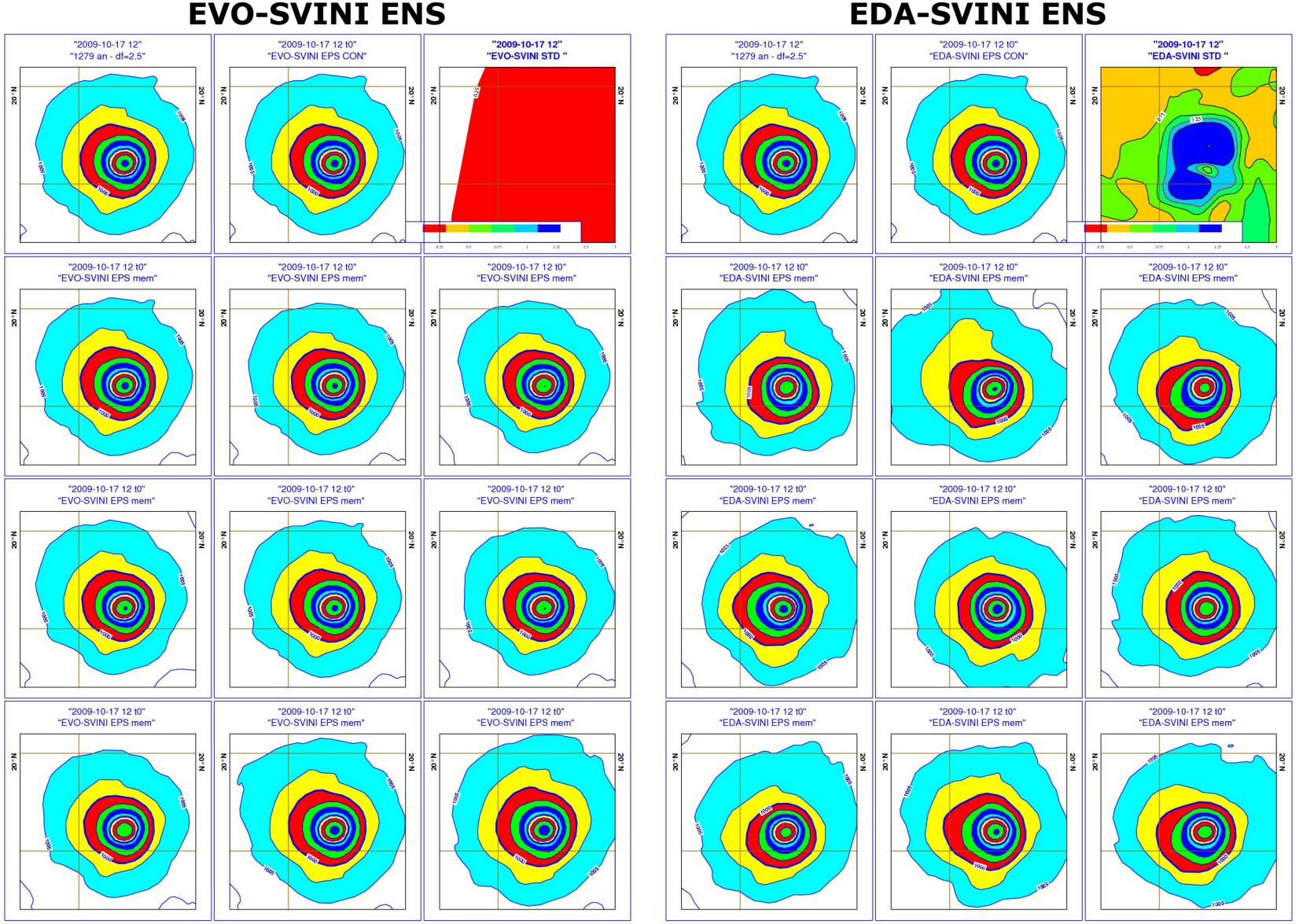

3. The EDA-SVINI ENS

The EDA-based perturbations are defined by differences between +6h forecasts:

$$PA_j(d,0) = A_j(d-6h,6h) - < A_j(d-6h,6h) >_{j=1,N_{EDA}}$$

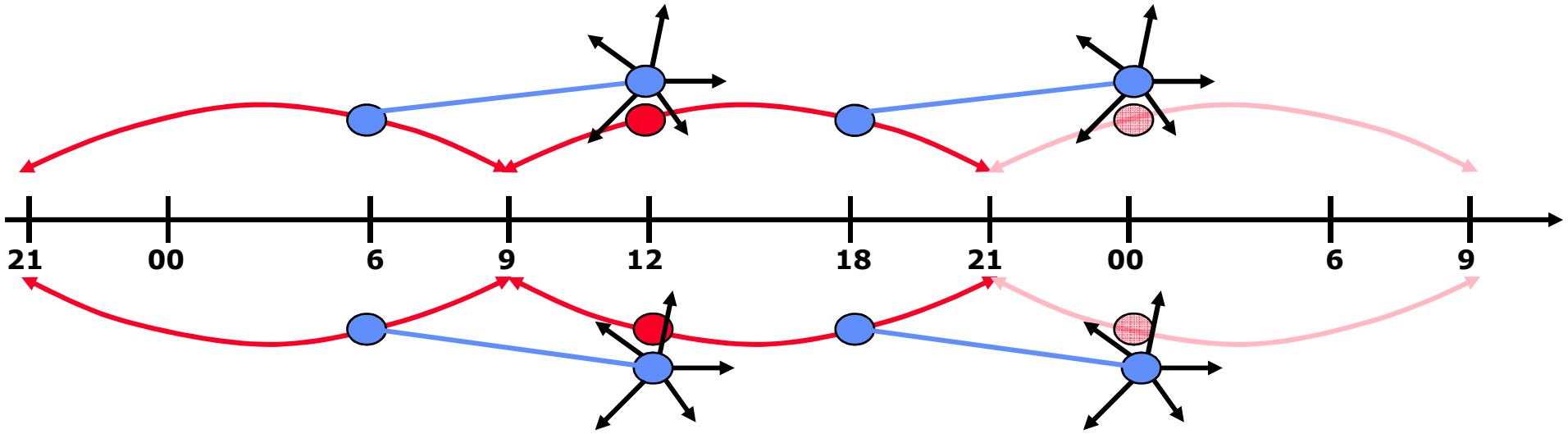

This choice is consistent with data-assimilation practice followed when computing J_b statistics. In operation, this allows ENS to start as soon as the control analysis (T_L1279L137) is available.

3. The EDA-SVINI ENS

The choice of using 6h forecasts from the EDA run during the previous DA cycle is consistent with the fact that the operational 48h-SVs are also computed starting from a 6-hour forecast, i.e. along a t+6h to t+54h trajectory:

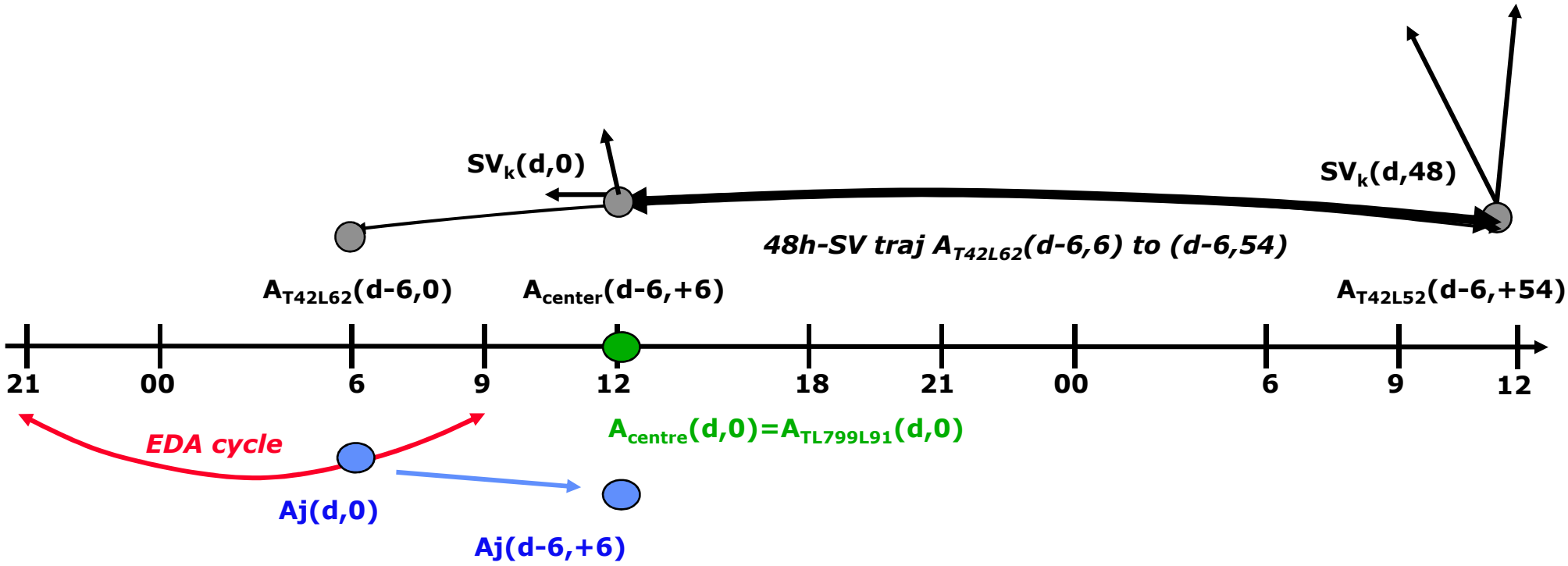

3. Spectra of EDA & SVINI ENS – TR 0/24h

The top figure shows the squared amplitude of the SVINI (red) and EDA (blue) perturbations in terms of T850 over the tropics at initial time. The bottom panel shows the same but for t+24h. Results have been averaged over 13 cases.

Results confirm that the SVINI ensemble has too little spread over the tropics.